Tetrahedron: *Asymmetry* 21 (2010) 1797–1815

Contents lists available at ScienceDirect

Tetrahedron: *Asymmetry*

journal homepage: www.elsevier.com/locate/tetasy

A systematic study of the solid state and solution phase conformational preferences of β-peptides derived from transpentacin

Elin Abraham [a], Callum W. Bailey [a], Timothy D. W. Claridge [a], Stephen G. Davies [a,*], Kenneth B. Ling [a], Barbara Odell [a], Thomas L. Rees [a], Paul M. Roberts [a], Angela J. Russell [a], Andrew D. Smith [a], Lorna J. Smith [b], Helen R. Storr [a], Miles J. Sweet [a], Amber L. Thompson [a], James E. Thomson [a], George E. Tranter [a,c], David J. Watkin [a]

[a] *Department of Chemistry, Chemistry Research Laboratory, University of Oxford, Mansfield Road, Oxford OX1 3TA, UK*
[b] *Department of Chemistry, Inorganic Chemistry Laboratory, University of Oxford, South Parks Road, Oxford OX1 3QR, UK*
[c] *Chiralabs Ltd, BCIE, Oxford University Begbroke Science Park, Sandy Lane, Yarnton, Oxfordshire OX5 1PF, UK*

ARTICLE INFO

Article history:
Received 20 May 2010
Accepted 27 May 2010
Available online 13 July 2010

Dedicated to Professor Henri Kagan on the occasion of his 80th birthday

ABSTRACT

The solid state and solution phase conformational preferences of a homologous series of β-peptides derived from (*S*,*S*)-2-aminocyclopentanecarboxylic acid (transpentacin) have been investigated using a variety of spectroscopic and crystallographic techniques. These studies indicate that the hexamer and pentamer persist as a 12-helix in both the solid state and solution phase. Although the conformational traits of a 12-helix are exhibited by oligomers with as few as three residues in the solid state, in solution the trimer exists as an equilibrium of many alternative conformers whilst the tetramer has been shown to predominantly exist in either a 12-helix or a turn-type conformation.

1. Introduction

β-Amino acids are an attractive moiety for the formation of peptidomimetics, whereby their replacement for specific α-amino acids in existing peptide compounds offers remarkable opportunities to mimic the action of these peptides whilst offering improved bioavailability and therapeutic lifetimes.[1] β-Peptides (i.e., those composed solely of β-amino acid residues) themselves display biological activities such as inhibition of fat and cholesterol absorption[2] and antibiotic properties,[3] and as such have been the subject of several investigations.[4] For instance, Seebach and co-workers reported their investigations into the conformational characterisation of the β^3-substituted hexapeptide **1** which adopts a 14-helix[5] conformation in organic solutions[1a,6] (Fig. 1). Gellman investigated the introduction of covalent constraints to pre-organise the molecule for specific secondary structure motifs without blocking the H-bonding sites along the peptide backbone. Hexamer **4**, assembled from residues of the β-amino acid (*R*,*R*)-2-aminocyclohexanecarboxylic acid (transhexacin) **2**, populates a 14-helix in both the solution and solid state,[7] whilst hexamer **5**, assembled from residues of the β-amino acid (*R*,*R*)-2-aminocyclopentanecarboxylic acid (ACPC or transpentacin) **3**, adopts a 12-helical conformation[7b,8,9] (Fig. 1). A variety of analogues have since been reported and analysed for the presence of secondary structural preferences.[10]

These previous studies have not, however, systematically investigated the effect of increasing transpentacin oligomer length on the predilection to adopt a 12-helix. Upon inspection of the 12-helix adopted by hexamer **5** we envisaged that this secondary structure motif could, in principle, be adopted by the corresponding transpentacin pentamer **7**, tetramer **8** and trimer **9** through the formation of three, two and one inter-residue 12-membered hydrogen bonds, respectively (Fig. 2).[11] In order to facilitate subsequent analysis of alkyl-substituted derivatives, our initial investigations set out to determine when a 12-helical motif is substantially populated within the progressively increasing transpentacin oligomeric series, or whether alternative conformations are accessible, in both the solid state and solution phase. It was envisaged that investigation of a range of protecting group strategies for the transpentacin oligomers may facilitate crystallisation and thus enable solid state investigations to be performed. The results of these investigations are disseminated herein.

2. Results and discussion

2.1. Asymmetric synthesis of transpentacin-derived oligomers

Initial studies into either an *N*-Boc/*O*-Me- or an *N*-Cbz/*O*-^{t}Bu-protecting group strategy revealed the latter to be more efficacious, and therefore multigram quantities of the requisite monomers **13** and **15** were prepared. β-Amino ester **12** was prepared on a >10 g scale following the previously described procedure.[12] Conjugate addition

* Corresponding author.
E-mail address: steve.davies@chem.ox.ac.uk (S.G. Davies).

0957-4166/$ - see front matter © 2010 Elsevier Ltd. All rights reserved.
doi:10.1016/j.tetasy.2010.06.001

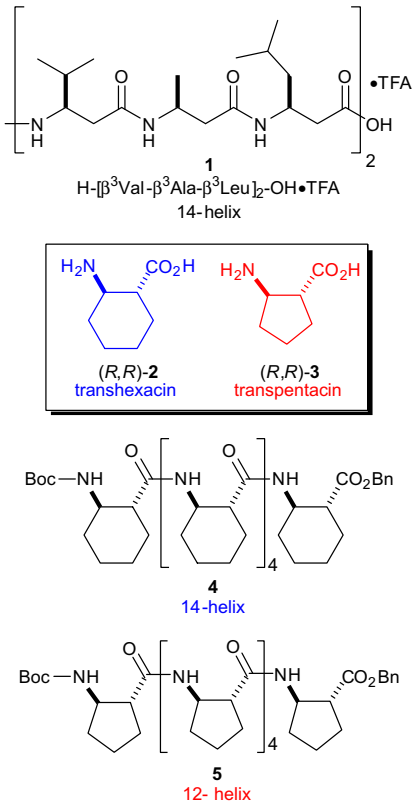

Figure 1. Structure of β^3-substituted hexamer **1**, transhexacin **2**, transpentacin **3** and their respective hexamers **4** and **5**.

of lithium (*S*)-*N*-benzyl-*N*-(α-methylbenzyl)amide to *tert*-butyl cyclopent-1-enecarboxylate **10** was followed by quenching with satd aq NH_4Cl, and treatment of the initially formed *cis*-diastereoisomer **11**[13] (87% yield, 96:4 dr) with KO^{t}Bu in dry ^{t}BuOH[14] gave the *trans*-diastereoisomer **12** in >99:1 dr, and as a white solid in 81% isolated yield after chromatographic purification.[15] Subsequent protecting group manipulation gave NH/*O*-^{t}Bu monomer ('monomer amine') **13** and *N*-Cbz/OH monomer ('monomer acid') **15**[16] in 92% and 62% yields over one and three steps, respectively, from **12** (Scheme 1).

Under optimised conditions, a fragment condensation approach to peptide synthesis was employed, utilising an HOBt/EDC·HCl-mediated coupling protocol in $CHCl_3$. Coupling of monomer amine **13** and monomer acid **15** afforded dimer **16** in 77% yield and >99:1 dr. Orthogonal N- and O-deprotection of dimer **16** was achieved using $Pd(OH)_2/C$ under H_2 (1 atm) and TFA, respectively, giving the corresponding dimer amine **17** and dimer acid **18** in 97% and 86% yields, respectively, and in >99:1 dr in each case, as crystalline solids. Trimer **19** was synthesised from monomer acid **15** and dimer amine **17** in 72% isolated yield and >99:1 dr, and was subsequently N-deprotected using $Pd(OH)_2/C$ under H_2 (1 atm) to afford the corresponding trimer amine **21** in 89% yield. Coupling of either dimer amine **17** or trimer amine **21** with dimer acid **18** ([2+2] and [2+3] fragment condensations, respectively) occurred with quantitative conversion in both cases giving tetramer **20** and pentamer **23** as single diastereoisomers >99:1 dr), in 73% and 56% yields, respectively, after column chromatography. The synthesis of hexamer **24** was achieved through hydrogenolysis of tetramer **20** to give the corresponding tetramer amine **22** in 89% yield, which was subsequently coupled with dimer acid **18** ([2+4] fragment condensation) to afford a mixture of products (85% conversion) that was purified to give hexamer **24** in 66% isolated yield (Scheme 2).

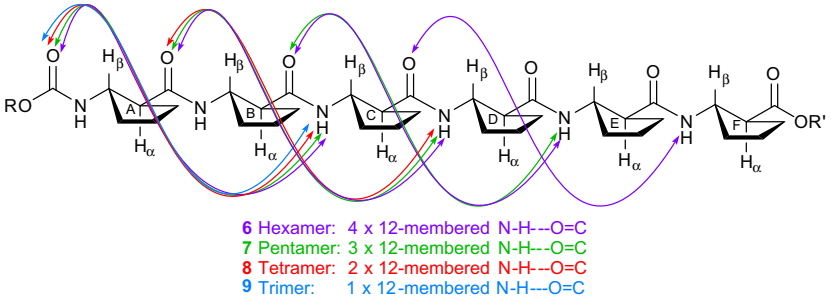

Figure 2. Potential 12-membered inter-residue hydrogen bonds within generic transpentacin hexamer **6**, pentamer **7**, tetramer **8** and trimer **9**.

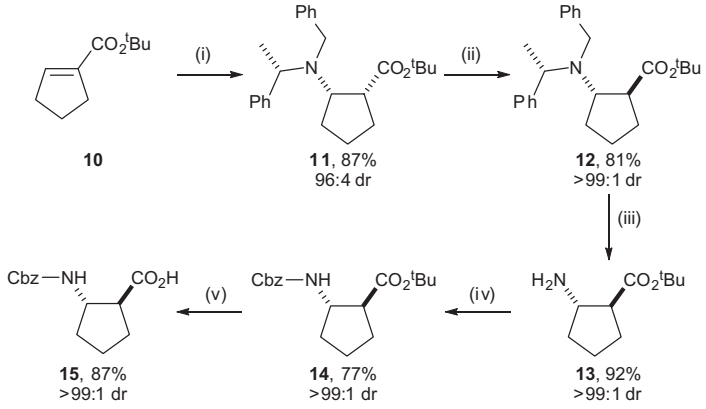

Scheme 1. Reagents and conditions: (i) lithium (*S*)-*N*-benzyl-*N*-(α-methylbenzyl)amide, THF, −78 °C, then NH_4Cl (satd aq), −78 °C to rt; (ii) KO^{t}Bu, ^{t}BuOH, reflux, 8 h; (iii) $Pd(OH)_2/C$, H_2 (5 atm), MeOH, rt, 16 h; (iv) CbzCl, Et_3N, THF, rt, 16 h; (v) TFA, CH_2Cl_2, 0 °C to rt, 3 h.

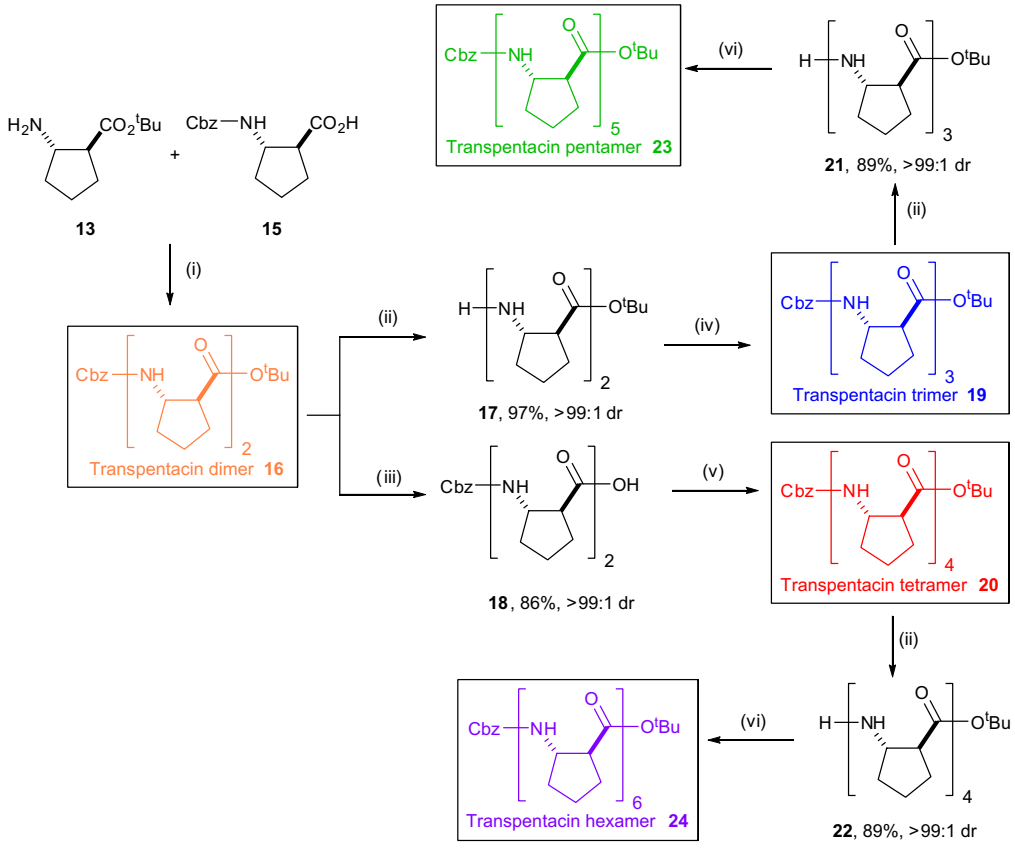

Scheme 2. Reagents and conditions: (i) EDC·HCl, HOBt, Et_3N, $CHCl_3$, rt, 16 h; (ii) $Pd(OH)_2/C$, H_2 (1 atm), MeOH, rt 16 h; (iii) TFA, CH_2Cl_2, 0 °C to rt, 12 h; (iv) monomer acid **15**, EDC·HCl, HOBt, Et_3N, $CHCl_3$, rt, 16 h; (v) dimer amine **17**, EDC·HCl, HOBt, Et_3N, $CHCl_3$, rt, 16 h; (vi) dimer acid **18**, EDC·HCl, HOBt, Et_3N, $CHCl_3$, rt, 16 h.

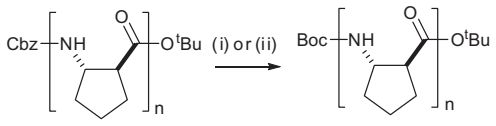

	n	Conditions	Product	Yield (dr) %
16	2 (dimer)	(i)	**25**	81 (>99:1)
19	3 (trimer)	(i)	**26**	80 (>99:1)
20	4 (tetramer)	(i)	**27**	65 (>99:1)
23	5 (pentamer)	(i)	**28**	61 (>99:1)
24	6 (hexamer)	(ii)	**29**	23 (>99:1)

Scheme 3. Reagents and conditions: (i) $Pd(OH)_2/C$, Boc_2O, H_2 (1 atm), MeOH, rt, 12 h; (ii) $Pd(OH)_2/C$, H_2 (1 atm), MeOH, rt, 12 h, then $NaHCO_3$, Boc_2O, MeOH,))), rt, 16 h.

Finally, to facilitate subsequent analysis by CD spectroscopy, the *N*-Cbz functionality within oligomers **16**, **19**, **20** and **23** was exchanged for an *N*-Boc-protecting group via hydrogenolysis mediated by $Pd(OH)_2/C$ in the presence of Boc_2O, giving the corresponding *N*-Boc/*O*-^{t}Bu-protected oligomers **25–28** in good yields. Transformation of hexamer **24** required hydrogenolysis and subsequent sonication in the presence of $NaHCO_3$ in MeOH to install the *N*-Boc group within **29** (Scheme 3).

2.2. Conformational analysis of transpentacin-derived oligomers

2.2.1. Solid state conformational preferences: single crystal X-ray analysis

A variety of crystallisation techniques were applied to the range of transpentacin β-peptides (fully protected oligomers [Cbz-$(ACPC)_n$-O^{t}Bu and Boc-$(ACPC)_n$-O^{t}Bu], N-deprotected oligomers [H-$(ACPC)_n$-O^{t}Bu] and O-deprotected oligomers [Cbz-$(ACPC)_n$-OH]). Single crystals of *N*-Boc/*O*-^{t}Bu hexamer **29**, *N*-Boc/*O*-^{t}Bu pentamer **28** and *N*-Boc/*O*-^{t}Bu tetramer **27** were produced and subjected to single crystal X-ray analyses which revealed the existence of a 12-helix motif in the solid state conformation of hexamer **29**, with four intramolecular hydrogen bonds observed, in accordance with the results of Gellman and co-workers.[7] Analysis of the solid state structures of pentamer **28** and tetramer **27** realised the prediction that these oligomers may also adopt a 12-helix motif through the presence of three and two intramolecular 12-membered H-bonds in the X-ray crystal structures of these two compounds, respectively (Figs. 3–5). All attempts to crystallise the fully protected trimer derivatives Cbz-$(ACPC)_3$-O^{t}Bu **19** and Boc-$(ACPC)_3$-O^{t}Bu **26** proved unsuccessful. However, a single crystal of trimer acid Cbz-$(ACPC)_3$-OH **30**[17] was produced and single crystal X-ray analysis revealed that the predicted 12-membered H-bonded ring was present in addition to an eight-membered C(O)O–H···O=C(B) interaction, involving the carboxylic acid group. It is postulated that this additional intramolecular H-bonded ring confers extra stability upon this motif not possible in the O-protected derivatives (Fig. 6).

The X-ray crystal structures of tetramer **27**, pentamer **28** and hexamer **29** were overlaid in order to compare the solid state conformations within these molecules. These results highlighted good parity between the three structures (Fig. 7).[18]

To date, the smallest fully protected transpentacin β-peptide to display a 12-helical conformation in the crystal lattice is *N*-Boc tetramer **27**, which is stabilised by only two intramolecular hydrogen bonds. Furthermore, the results of these solid state investigations suggest that oligomers derived from transpentacin have a strong predisposition to adopt the 12-helical motif, conformational traits

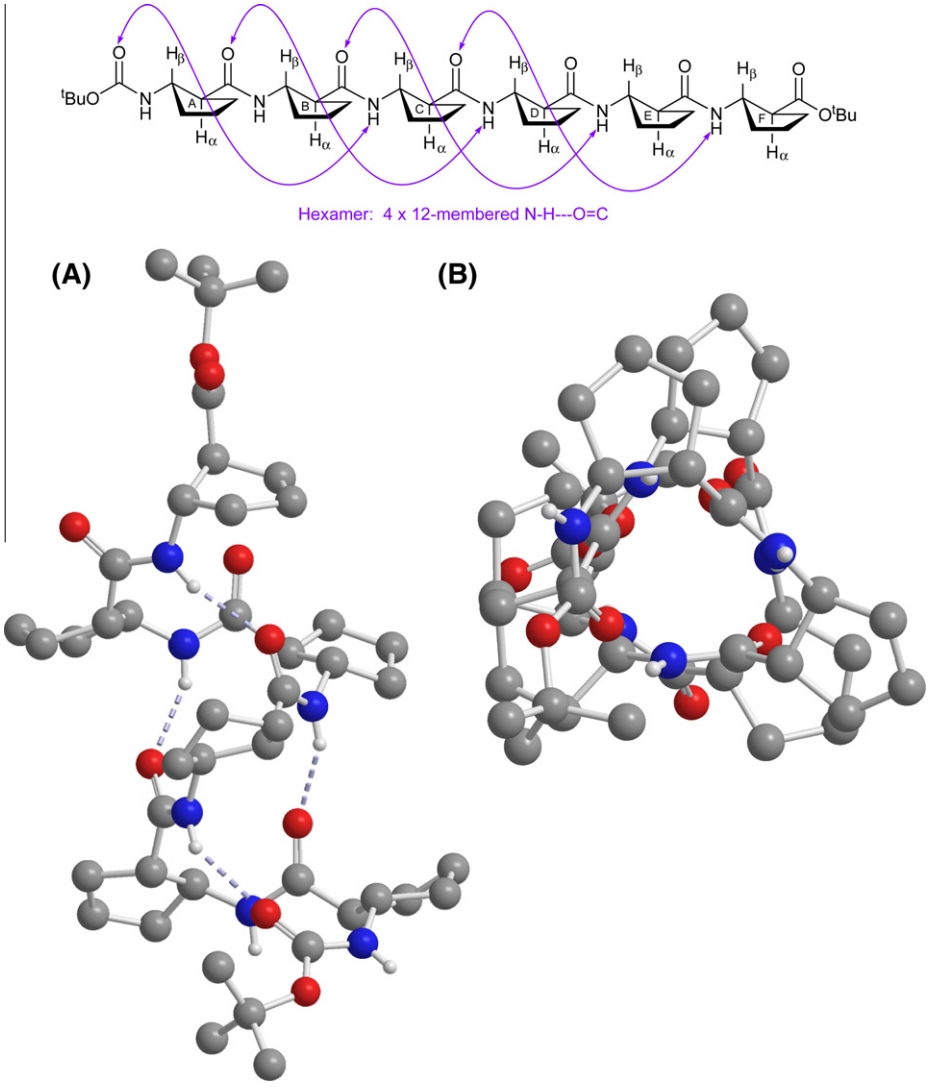

Figure 3. Chem-3D representation of the X-ray crystal structure of hexamer Boc-(ACPC)$_6$-O^{t}Bu **29**: (A) perpendicular to and (B) along the helical axis (some H atoms omitted for clarity).

of which are exhibited by molecules containing as few as three residues, as demonstrated through analysis of trimer acid **30**. With these promising results in hand, attention focused upon whether these observed folding preferences in the smaller β-peptides are manifested in solution, or if alternative conformers or irregular structures are populated.

2.2.2. Solution phase conformational preferences

Solution phase NMR studies were carried out on a range of transpentacin oligomers harbouring varying protecting groups: *N*-Cbz/*O*-^{t}Bu (trimer to hexamer **19**, **20**, **23** and **24**), *N*-Boc/*O*-^{t}Bu (trimer to hexamer **26–29**) and *N*-Cbz/OH (trimer **30**). Initial investigations sought to fully assign the primary structure of each oligomer, utilising a combination of 2D COSY, edited HSQC and TOCSY experiments. Additionally, 1D TOCSY experiments were also an asset when chemical shift overlap was problematic, allowing isolation of an individual ring system by transfer from the NH proton, and sequential assignments were performed using NOESY and ROESY spectra.[19] Boc-(ACPC)$_6$-OBn hexamer **5** has previously been shown by Gellman to adopt the 12-helix secondary structural motif in solution phase and solid state.[7] In the 12-helix, each NH proton [except NH(A)] has been shown to give rise to two strong, through space NOE correlations to two C$_\alpha$H protons (of residues i and $i-1$). In order to verify that the 12-helical conformation persisted in solution for Cbz-(ACPC)$_6$-O^{t}Bu hexamer **24** (which showed better resonance dispersion in $CDCl_3$ than Boc-(ACPC)$_6$-O^{t}Bu hexamer **29**) a full tabulation of NOE correlations was sought. Tr-ROESY data for hexamer **24** were acquired, giving rise to a number of long range inter-residue NOEs. The NH(i)→C$_\alpha$H(i) and NH(i)→C$_\alpha$H($i-1$) pattern of NOEs, characteristic of the 12-helix, was observed within hexamer **24**. Two sets of long range correlations were also recorded: C$_\beta$H(i)→C$_\alpha$H($i+2$) and C$_\beta$H(i)→NH($i+2$), which are also indicative of a 12-helix motif[7b] (Fig. 8).

With these data in hand, structure calculations were performed for the hexamer **24** with XPLOR, using distance restraints from the experimental ^{1}H NMR NOE data.[20] A simulated annealing protocol[21] was employed and an ensemble of 20 structures was calculated. All these structures contained the 12-membered hydrogen bonds *CO*(A)→N*H*(D), *CO*(B)→N*H*(E) and *CO*(C)→N*H*(F) and were further refined with distance restraints for these hydrogen bonds included. An overlay of the 10 lowest energy structures thus generated showed remarkable parity; this suggests that the produced structures offer an accurate representation of the solution phase conformation of hexamer **24**, and thus substantiates the existence of a 12-helix motif for this compound in solution (Fig. 9). When the lowest energy calculated NMR structure of hexamer **24** was

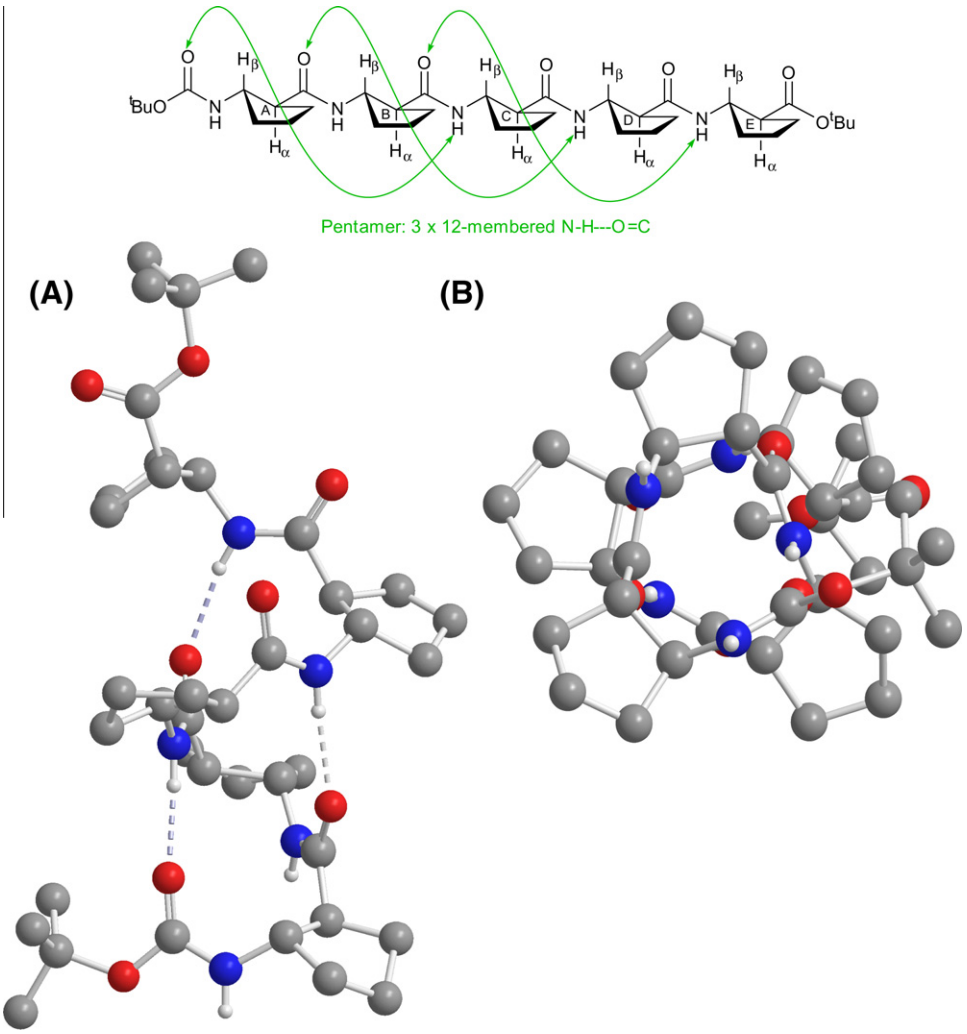

Figure 4. Chem-3D representation of the X-ray crystal structure of pentamer Boc-(ACPC)$_5$-O^{t}Bu **28**: (A) perpendicular to and (B) along the helical axis (some H atoms omitted for clarity).

overlaid with the solid-state X-ray crystal structure of hexamer **29**, excellent agreement was noted, which suggests that the 12-helix is favoured for hexamers **24** and **29** in both the solid state and solution phase (Fig. 9). Further affirmation of this assertation was obtained from the IR spectrum of hexamer **29** at high dilution (2 mM), which revealed two peaks associated with N–H bonds. A sharp peak at 3439 cm^{-1} was indicative of a non-hydrogen bonding situation: in a 12-helix NH(A) and NH(B) would be able only to participate in intermolecular hydrogen bonds but at such high dilution this is unlikely and it is therefore possible that these two protons are responsible for this sharp peak. A second, broader peak centred on 3326 cm^{-1} is indicative of intramolecular hydrogen bonding, which may be ascribed to the environments of NH protons (C)–(F) within a 12-helix.

The 12-helix solid-state X-ray crystal structure of Boc-(ACPC)$_5$-O^{t}Bu pentamer **28** exhibited three C*O*(i)→N*H*(i + 3) intramolecular hydrogen bonds involving N*H* protons (C)–(E) and it was therefore envisaged that if this motif persisted in solution, the equivalent key NOE correlations reported by Gellman for hexamer **5**[7b] would also be present within pentamer **28**. Unlike Boc-(ACPC)$_6$-O^{t}Bu hexamer **29**, Boc-(ACPC)$_5$-O^{t}Bu pentamer **28** displayed good resonance dispersion in $CDCl_3$ and therefore this oligomer was investigated to facilitate direct comparison of the solid state and solution phase structures. A set of NOEs were produced for pentamer **28** that contained all the characteristic correlations for a 12-helix, although some could not be unambiguously assigned a relative intensity due to resonance overlap: two of the three $H_\beta(i)$–NH(i + 2) correlations were unambiguously assigned, as were two of the three $H_\beta(i)$–$H_\alpha(i+2)$ correlations, with the remainder being present although non-quantifiable (Fig. 10).

Structure calculations using the NOEs for pentamer **28** were performed in an analogous fashion to those previously described for hexamer **24**. All 20 of the NMR structures contained the 12-membered hydrogen bonds C*O*(A)→N*H*(D) and C*O*(B)→N*H*(E), and so the structures were further refined with distance restraints for these hydrogen bonds included. The 10 lowest energy structures were superimposed, affording a conformation that closely resembled a 12-helix (Fig. 11). Good agreement with the solid-state X-ray crystal structure was again observed. The IR spectrum of pentamer **28** showed a sharp non-hydrogen bonding stretch at 3436 cm^{-1} and a broader peak centred on 3336 cm^{-1} with a shoulder at 3271 cm^{-1}, suggesting both inter- and intramolecular hydrogen bonding N–H stretches. Taken together, these results suggest that the 12-helix represents a dominant conformation for pentamer **28** in solution, although an alternative conformation may be partially adopted.

Analysis of the Tr-ROESY spectrum for tetramer **27** revealed the presence of a large number of inter-residue NOEs, some of which

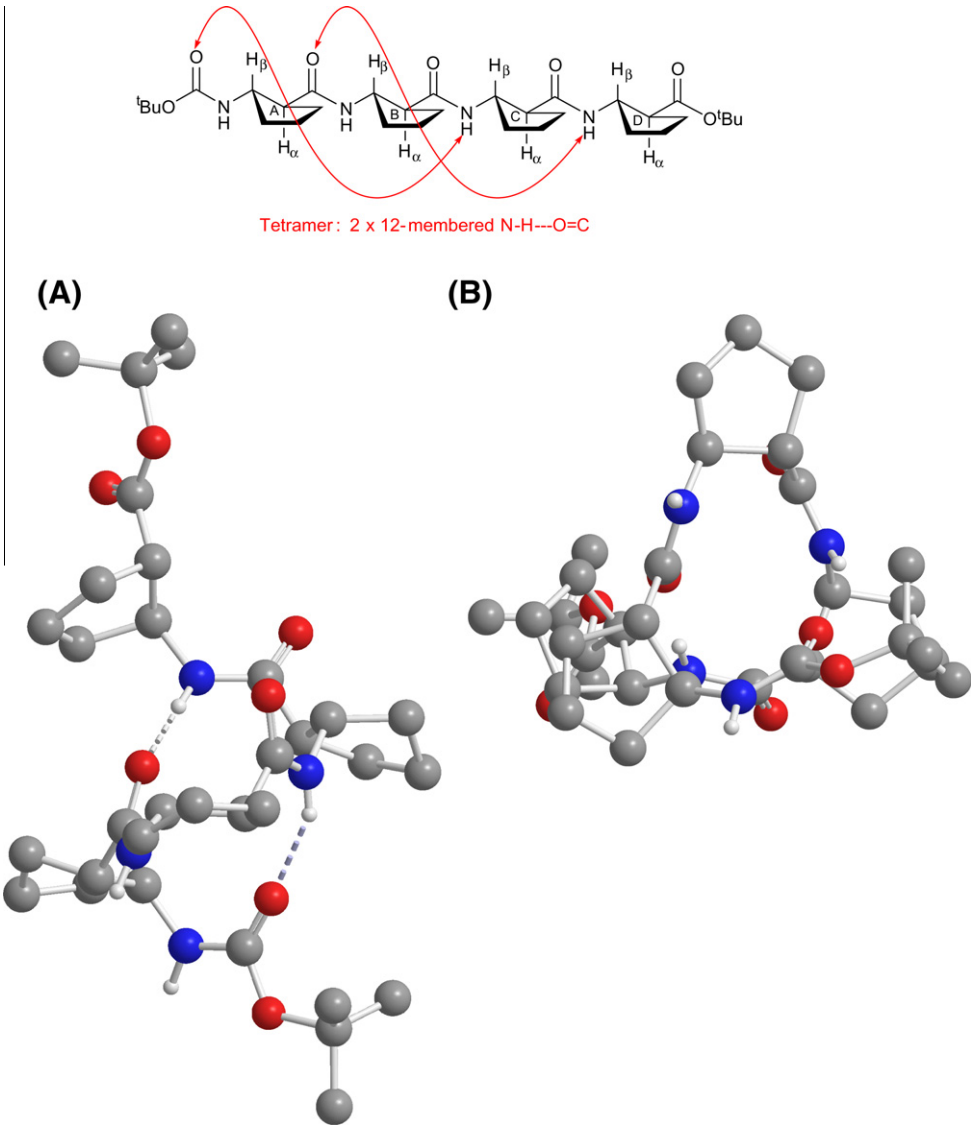

Figure 5. Chem-3D representation of the X-ray crystal structure of tetramer Boc-(ACPC)$_4$-O^{t}Bu **27**: (A) perpendicular to and (B) along the helical axis (some H atoms omitted for clarity).

were characteristic of a 12-helical motif being present in solution (Fig. 12). Structure calculations were performed for tetramer **27** using the experimental NOE data and the same simulated annealing protocol, but without the inclusion of any hydrogen bond restraints. The resultant NMR structures revealed that conformation of tetramer **29** is less well defined than that of the hexamer **24** or pentamer **28**. Some of the generated structures contained the 12-membered hydrogen bond CO(A)→NH(D) as observed in the crystal structure, but in other structures this was replaced with an eight-membered hydrogen bond CO(A)→NH(C), indicating an alternative turn-type conformation. The IR spectrum of tetramer **29** was indicative of two possible types of N–H stretch. In the N–H hydrogen bonding region, there are two distinct peaks (at 3273 and 3340 cm^{-1}), suggesting that there is more than one type of hydrogen bonding occurring. A sharper, non-hydrogen bonding peak at 3438 cm^{-1} is also noted. On diluting the sample 10-fold, much of the character from the original tetramer IR still remains, suggesting most of the hydrogen bonding in this oligomer is intramolecular. These studies suggest that this oligomer may populate multiple conformations in solution, of which the 12-helix may be only one possibility (Fig. 13).

2.2.3. Comparisons across the oligomer series

Analysis of the N–H ^{1}H NMR chemical shifts within the series of Cbz-(ACPC)$_n$-O^{t}Bu oligomers **19**, **20**, **23** and **24** and Boc-(ACPC)$_n$-O^{t}Bu oligomers **26–29** showed similar trends, which provided information about hydrogen bonding chemical environments (Fig. 14). In the Boc-(ACPC)$_n$-O^{t}Bu oligomers **27–29** (tetramer to hexamer), the chemical shift values of NH(C), NH(D), NH(E) and NH(F) (where relevant) are all very deshielded, appearing within the narrow range of 7.30–8.26 ppm in both homologous oligomer series, suggesting significantly similar hydrogen bonding chemical environments, likely to be intramolecular: it is intramolecular hydrogen bonding involving these protons that stabilises the 12-helical motif of **27–29** in both the X-ray crystal structures and solution phase energy-minimised NMR models. Conversely, the ^{1}H NMR chemical shift (and hence chemical environment) of the carbamate NH(A) protons was noted to be largely independent of oligomer length, appearing in the range 4.67–4.94 ppm as the trimer **26** to hexamer **29** series is traversed, suggesting that the hydrogen bonding environment of all NH(A) protons is similar. The chemical shift of NH(B) showed the greatest change upon increasing oligomer length, suggesting a considerable change in hydrogen bonding

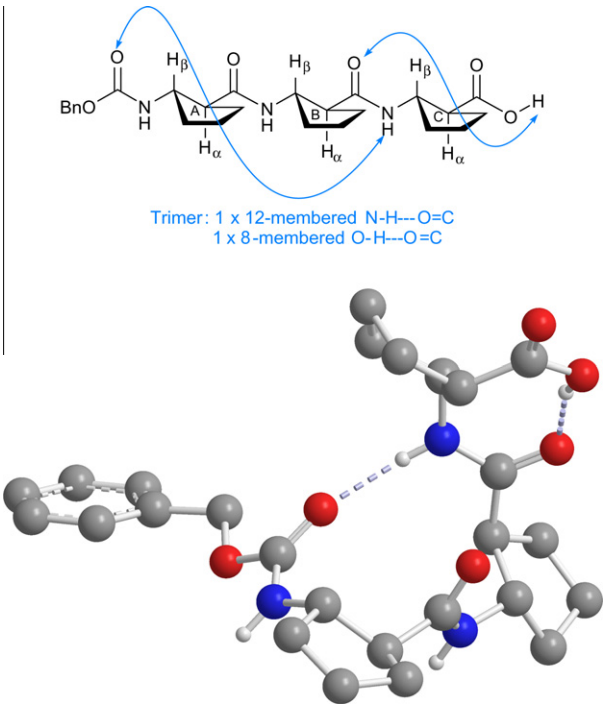

Figure 6. Chem-3D representation of the X-ray crystal structure of trimer Cbz-(ACPC)$_3$-OH **30** (some H atoms omitted for clarity).

environment, with the largest difference noted between the tetramer **27** and pentamer **28**. When DMSO-d_6 was added to a solution of pentamer **23** and hexamer **24** in $CDCl_3$ (26 mM), the volume of DMSO-d_6 added showed relatively little perturbation upon the shifts of amide protons N*H*(C)–N*H*(F) (where relevant), indicating that these protons are effectively shielded from the strong H-bonding solvent, consistent with their involvement in strong, intramolecular hydrogen bonds. Amide protons N*H*(A) and N*H*(B) displayed high sensitivity towards the presence of DMSO-d_6, suggesting that they are predominantly solvent exposed. An analogous study conducted on tetramer **20** did not display similar trends, with only N*H*(A) displaying a significant change in chemical shift with the addition of DMSO-d_6. These data suggest that the shorter oligomers (trimer, tetramer) have N*H*(C) and N*H*(D) involved in intramolecular hydrogen bonds, but the N-terminus of the molecule can adopt a conformation in which N*H*(B) can also form an intramolecular hydrogen bond. The population of such alternative conformers is depleted as the length of the oligomer increases and the 12-helix becomes the dominant conformation in which N*H*(A) and N*H*(B) remain solvent exposed.

These observations are consistent with pentamer **28** (but not necessarily tetramer **27**) showing a strong preference to adopt the 12-helix conformation in solution, which does not involve an intramolecular hydrogen bond to N*H*(B). To investigate this postulate further, the dependence of the N*H* chemical shift values on concentration was probed. N*H*(A) and N*H*(B) in both pentamers **23** and **28** and both hexamers **24** and **29** exhibited the greatest concentration dependence, whilst N*H*(C), N*H*(D), N*H*(E) and N*H*(F) exhibited negligible concentration dependence upon their chemical shift values, suggesting that the former partake in intermolecular hydrogen bonding between molecules. Determination of the temperature coefficients ($\Delta\delta_{NH}/\Delta T$ in ppb K^{-1}) of the amide protons of hexamer **24** revealed that at low concentrations (7 mM), N*H*(B) produced the lowest value, indicating that the environment of this proton remains constant throughout the temperature range. Increasing the concentration produces a corresponding increase in the coefficients for this residue and for N*H*(A), whereas those for N*H*(C)–N*H*(F) remain constant. Pentamer **23** and tetramer **20** exhibited a trend akin to that observed within hexamer **24**: with increasing concentration, the values recorded for protons N*H*(A) and N*H*(B) displayed the greatest increase. However, the data produced for tetramer **20** are not typical of a 12-helix conformation with N*H*(B) displaying the lowest values within the data set, and the only variation in concentration occurring with N*H*(A). This suggests that intramolecular hydrogen bonding behaviour is observed with N*H*(B) in shorter oligomers (Fig. 15).

Gellman et al. have produced experimentally derived CD traces of their transpentacin hexamer **5** (in the opposite enantiomeric series to **24** and **29**). These investigations demonstrated that experimentally the 12-helix secondary structure motif displays a CD signature in MeOH-d_3 with a reported positive-maximum at 204 nm, zero crossing at 214 nm and negative-maximum at 221 nm.[8] CD spectroscopy was performed on the transpentacin *N*-Boc series (dimer **25**→hexamer **29**) as solutions in TFE. The slight discrepancy between the data obtained from these experiments and with Gellman's reported data is likely due to the effects of different concentrations and solvents between the two systems. Comparison of these data indicated that *N*-Boc pentamer **28** and hexamer **29** show good correlation with the values reported by Gellman (λ_{+max} = 219 nm for both compounds, λ_0 = 210 and 211 nm, λ_{-max} = 200 and 202 nm, respectively), thus supporting the presence of a 12-helix conformation for these oligomers. The values recorded for *N*-Boc tetramer **27**, however, do not fit well (λ_{+max} = 216 nm, λ_0 = 206 nm and λ_{-max} = 198 nm), indicating that the 12-helix may not be the most highly populated conformation of this molecule in solution and other competing conformations (regular or irregular) may be present. The traces obtained for *N*-Boc dimer **25** and *N*-Boc trimer **26** display negative maxima at ca. 190 nm, which is characteristic of an irregular conformation for many peptide systems. These results suggest that a noticeable preference for a 12-helical conformation in solution occurs between the tetramer→pentamer transition, whilst the conformational ensemble of the lower oligomers could potentially include partially 12-helical and alternative conformers and irregular structures that inter-convert rapidly (Fig. 16).

3. Conclusion

In conclusion, β-peptides derived from (*S*,*S*)-2-aminocyclopentanecarboxylic acid (transpentacin) show a strong predisposition to adopt a 12-helix secondary structure, with the conformational traits of the 12-helix being exhibited by oligomers with as few as three residues in the solid state. The hexamer and pentamer persist as a 12-helix in solution phase, although in solution the tetramer appears to exist as an equilibrium of several different conformers, of which the 12-helix is one. Investigations into the ability of the 12-helix to tolerate alkyl substituents on the cyclopentane backbone are currently in progress in our laboratory.

4. Experimental

4.1. General experimental

All reactions involving organometallic or other moisture-sensitive reagents were carried out under a nitrogen or argon atmosphere using standard vacuum line techniques and glassware that was flame dried and cooled under nitrogen before use. Solvents were dried according to the procedure outlined by Grubbs and co-workers.[22] Other solvents and reagents were used as supplied (analytical or HPLC grade) without prior purification. Organic layers were dried over $MgSO_4$. Thin layer chromatography was performed

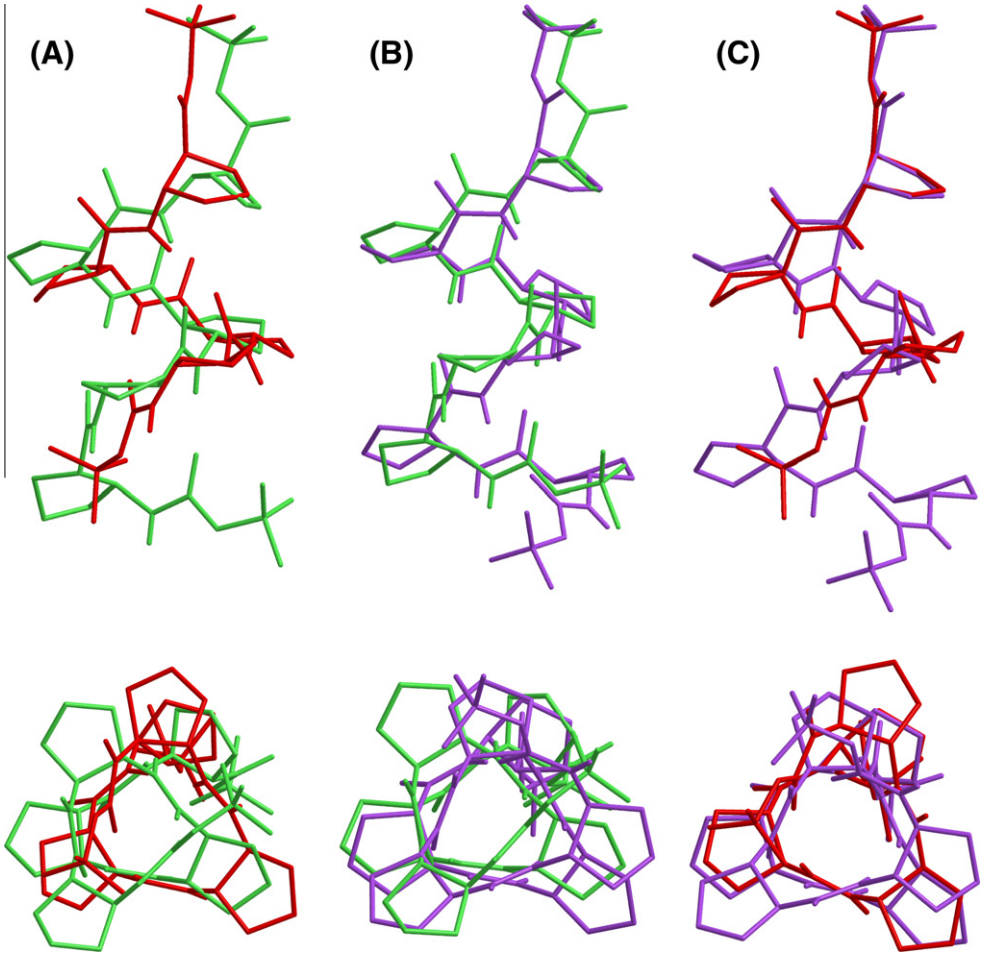

Figure 7. Chem-3D overlays of the X-ray crystal structures of tetramer **27** (red), pentamer **28** (green) and hexamer **29** (purple), perpendicular to and along the helical axis: (A) tetramer **27** versus pentamer **28**; (B) pentamer **28** versus hexamer **29**; (C) tetramer **27** versus hexamer **29**.

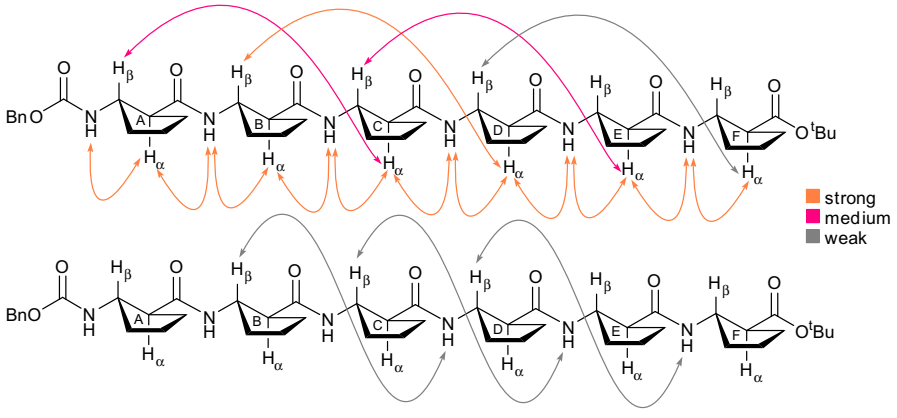

Figure 8. Summary of the resolved intra- and inter-residue NOEs observed in hexamer **24**.

on aluminium plates coated with 60 F_{254} silica. Plates were visualised using UV light (254 nm), iodine, 1% aq $KMnO_4$ or 10% ethanolic phosphomolybdic acid. Flash column chromatography was performed on Kieselgel 60 silica on a glass column, or on a Biotage SP4 automated flash column chromatography platform.

Elemental analyses were recorded by the microanalysis service of the Inorganic Chemistry Laboratory, University of Oxford, UK. Melting points were recorded on a Gallenkamp Hot Stage apparatus and are uncorrected. Optical rotations were recorded on a Perkin–Elmer 241 polarimeter with a water-jacketed 10 cm cell. Specific rotations are reported in 10^{-1} deg cm^2 g^{-1} and concentrations in g/100 mL. IR spectra were recorded on a Bruker Tensor 27 FT-IR spectrometer as either a thin film on NaCl plates (film) or a KBr disc (KBr), as stated. Selected characteristic peaks are reported in cm^{-1}. NMR spectra were recorded on Bruker Avance spectrometers in the deuterated solvent stated. Spectra were recorded at rt

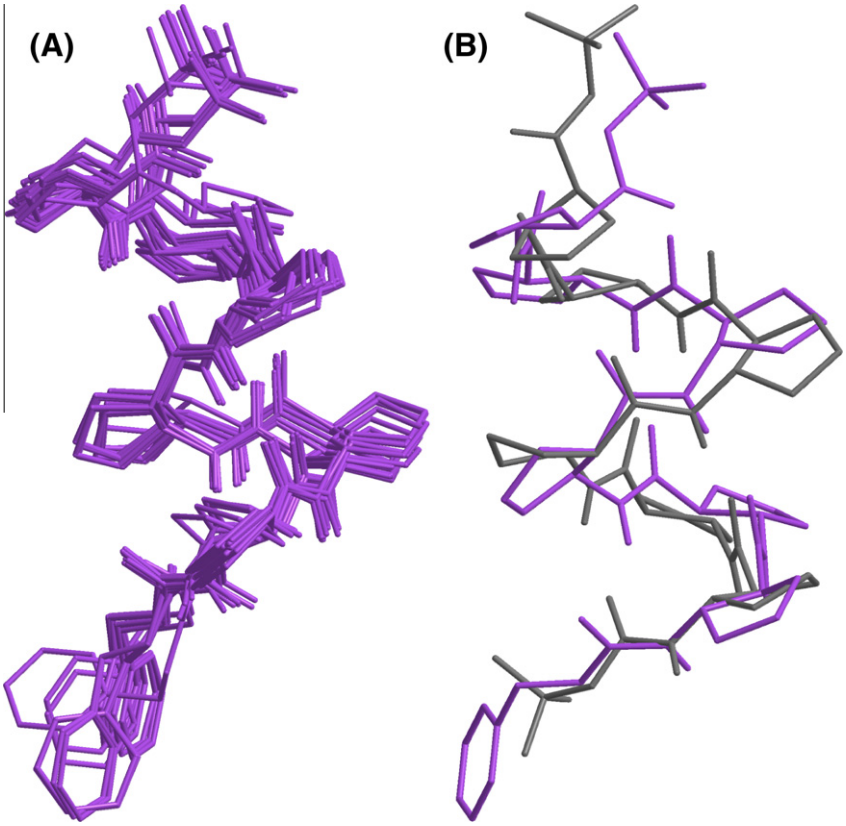

Figure 9. (A) Overlay of the 10 lowest energy NMR structures of hexamer **24** viewed perpendicular to the helical axis; (B) overlay of the lowest energy NMR structure of hexamer **24** (purple) and the X-ray crystal structure of hexamer **29** (grey) viewed perpendicular to the helical axis.

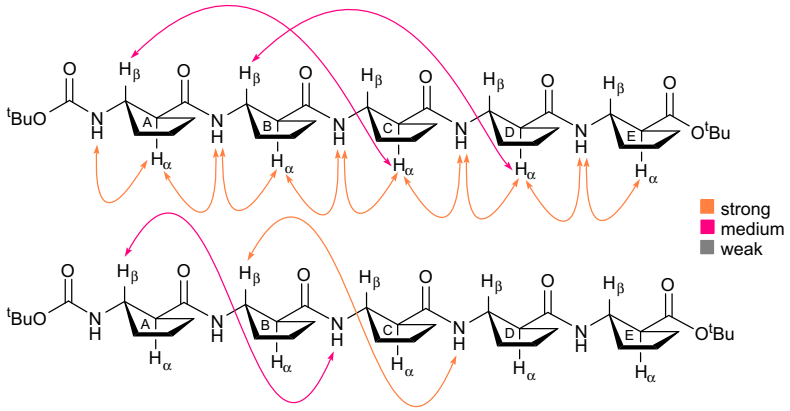

Figure 10. Summary of the resolved intra- and inter-residue NOEs observed in the transpentacin pentamer **28**.

unless otherwise stated. The field was locked by external referencing to the relevant deuteron resonance. Low-resolution mass spectra were recorded on either a VG MassLab 20–250 or a Micromass Platform 1 spectrometer. Accurate mass measurements were run on either a Bruker MicroTOF internally calibrated with polyalanine, or a Micromass GCT instrument fitted with a Scientific Glass Instruments BPX5 column (15 m × 0.25 mm) using amyl acetate as a lock mass.

4.2. General experimental procedures

4.2.1. General procedure 1 for N-deprotection

$Pd(OH_2)/C$ was added to a stirred, degassed solution of the requisite amine in MeOH. The resulting suspension was stirred under H_2 for 16 h, after which time the reaction mixture was filtered through Celite® (eluent MeOH) and concentrated in vacuo.

4.2.2. General procedure 2 for O-deprotection

TFA was added to a stirred solution of the requisite *tert*-butyl ester in CH_2Cl_2 at 0 °C. The reaction mixture was allowed to warm to rt and stirred for 3 h before being concentrated in vacuo and dried under high vacuum.

4.2.3. General procedure 3 for HOBt/EDC·HCl-mediated peptide coupling[23]

A stirred solution of the requisite amine in $CHCl_3$ was successively treated with Et_3N, HOBt, the requisite carboxylic acid and EDC·HCl. After 16 h, the reaction mixture was washed sequentially

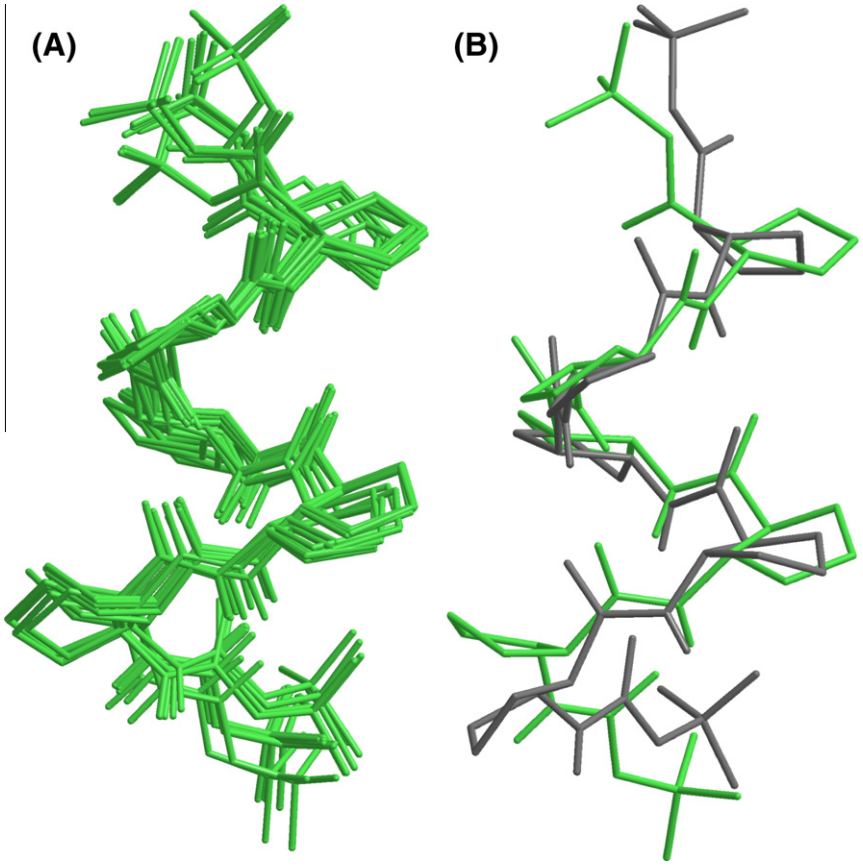

Figure 11. (A) Overlay of the 10 lowest energy NMR structures of **28** viewed perpendicular to the helical axis; (B) overlay of the lowest energy NMR structure (green) and the X-ray crystal structure (grey) of **28** viewed perpendicular to the helical axis.

with 1 M aq HCl, satd aq $NaHCO_3$ and brine and then dried and concentrated in vacuo.

4.2.4. General procedure 4 for N-protecting group swap (*N*-Cbz→*N*-Boc)

$Pd(OH_2)$/C was added to a stirred, degassed solution of the requisite *N*-Cbz protected amine and Boc_2O in MeOH. The resulting suspension was stirred under H_2 (1 atm) for 16 h, after which time the reaction mixture was filtered through Celite® (eluent MeOH) and concentrated in vacuo.

4.3. *tert*-Butyl cyclopent-1-enecarboxylate 10

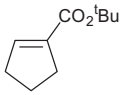

A solution of adipoyl chloride (600 g, 3.28 mol) in Et_2O (1.2 L) was added dropwise to a solution of ^{t}BuOH (941 mL, 9.83 mol) and *N*,*N*-dimethylaniline (1.25 L, 9.83 mol) in Et_2O (2.4 L) at 0 °C. The resultant mixture was allowed to warm slowly to rt and stirred for 24 h. The solution was diluted with H_2O (1.5 L) and the aqueous phase was separated. The organic portion was washed sequentially with 1 M aq HCl (5 × 500 mL), satd aq $NaHCO_3$ (1 L) and brine (1 L), then dried and concentrated in vacuo to give di-*tert*-butyl adipate as a colourless oil that crystallised on standing (694 g, 82%);[24] mp 29–30 °C; {lit.[24] mp 29–31 °C}; δ_H (400 MHz, $CDCl_3$) 1.43 (18H, s, 2 × CMe_3), 1.58–1.68 (4H, m, C(3)H_2, C(4)H_2), 2.20–2.23 (4H, m, C(2)H_2, C(5)H_2).

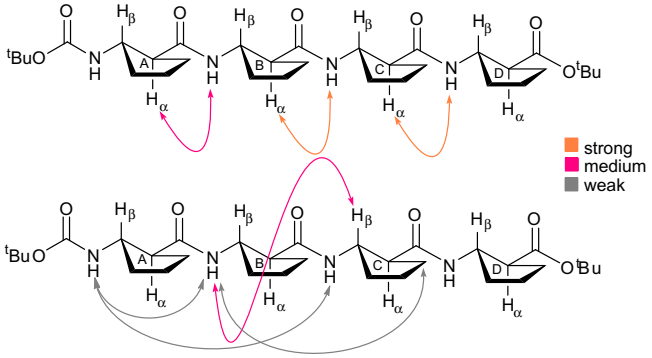

Figure 12. Summary of the resolved intra- and inter-residue NOEs observed in the transpentacin tetramer **27**.

NaH (60% suspension in mineral oil, 72.5 g, 1.80 mol) was suspended in PhMe (1.6 L) and the resultant mixture was heated to 60 °C. A solution of di-*tert*-butyladipate (2.60 g, 0.01 mol) in ^{t}BuOH (10 mL) was added via syringe. After 30 min, more di-*tert*-butyladipate (232 g, 0.90 mol) as a solution in PhMe (300 mL) was added dropwise. The resultant mixture was heated at 100 °C for 3 h, then allowed to cool to rt before being cooled to 0 °C prior to the sequential addition of MeOH (25 mL), H_2O (25 mL) and satd aq NH_4Cl (250 mL). The organic layer was separated, dried and concentrated in vacuo. Purification via vacuum distillation gave *tert*-butyl 2-oxocyclopentanecarboxylate as a colourless oil (122 g, 73%);[25] bp 110–112 °C (7.5 mmHg); δ_H (400 MHz, $CDCl_3$) 1.45 (9H, s, CMe_3), 1.79–1.90 (1H, m, C(4)H_A), 2.07–2.31 (5H, m, C(3)H_2, C(4)H_B, C(5)H_2), 3.05 (1H, app t, *J* 8.8, C(1)*H*).

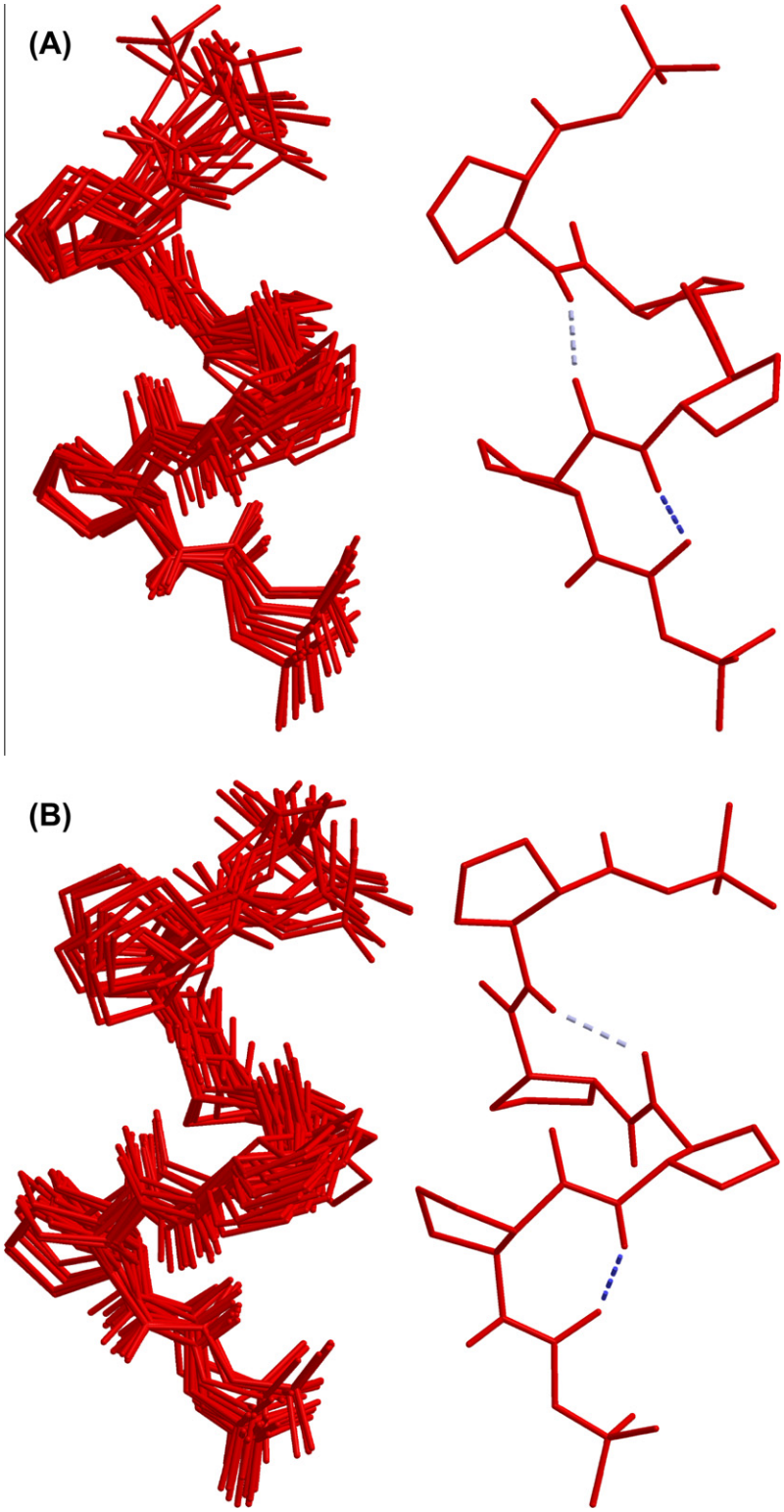

Figure 13. (A) Overlay of the 10 lowest energy NMR structures of tetramer **27**, containing a 12-membered ring hydrogen bond N(D)–H···O═C(A), viewed perpendicular to the helical axis; (B) Overlay of the 10 lowest energy NMR structures of tetramer **27**, containing an eight-membered ring hydrogen bond N(C)–H···O═C(A), viewed perpendicular to the helical axis.

$NaBH_4$ (15.6 g, 0.41 mol) was added portionwise to a solution of *tert*-butyl 2-oxocyclopentanecarboxylate (76.0 g, 0.41 mol) in EtOH (1 L) at 0 °C. The reaction mixture was allowed to warm to rt and the progress of the reaction was monitored by TLC. Once all the starting material had been consumed the reaction was cooled to 0 °C before the dropwise addition of H_2O until the resultant solid aggregated, followed by the addition of excess satd aq NH_4Cl (1 L). The mixture was diluted with Et_2O (1 L), the layers were separated and the aqueous layer was extracted with Et_2O (3 × 1 L). The combined organic layers were dried and concentrated in vacuo. The residue was dissolved in CH_2Cl_2 (1 L), cooled to 0 °C, and Et_3N (387 mL, 2.77 mol) and DMAP (4.84 g, 39.6 mmol)

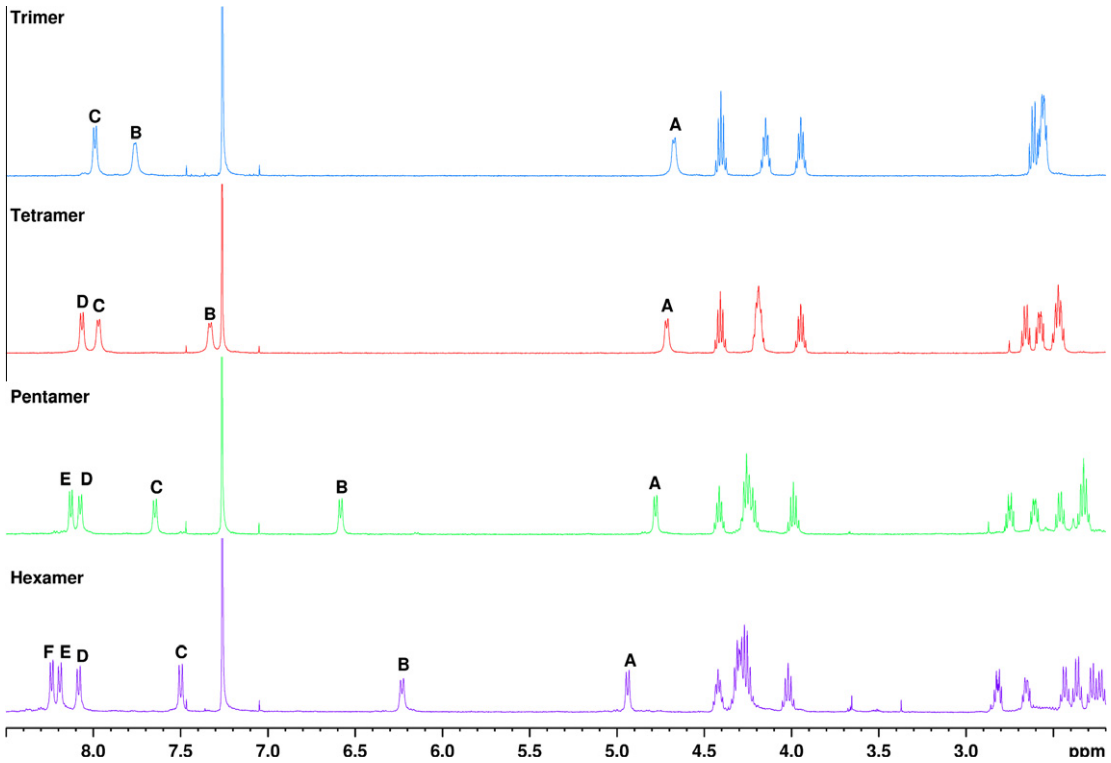

Figure 14. ^{1}H NMR spectra of Boc-(ACPC)$_n$-O^{t}Bu oligomers **26–29** [trimer (n = 3) to hexamer (n = 6)] at 298 K in $CDCl_3$. N*H* protons are labelled from the N-terminus. Peaks between 4.00 and 4.50 ppm are due to H_β protons, and those between 2.00 and 3.00 ppm are due to H_α protons.

were added, followed by the dropwise addition of a solution of MsCl (123 mL, 1.58 mol) in CH_2Cl_2 (500 mL). The resultant mixture was stirred at 0 °C for 1 h before being allowed to warm slowly to rt. The reaction mixture was stirred at rt for a further 8 h before the addition of H_2O (1.5 L). The layers were separated and the organic layer was washed sequentially with 1 M aq HCl (1 L), H_2O (1 L), satd aq $NaHCO_3$ (1 L) and brine (1 L), then dried and concentrated in vacuo. The residue was dissolved in CH_2Cl_2 (1 L), cooled to 0 °C, and a solution of DBU (79.1 mL, 0.53 mol) in CH_2Cl_2 (79.1 mL) was added dropwise. After 4 h, the reaction mixture was washed sequentially with 1 M aq HCl (1 L) and brine (1 L), then dried and concentrated in vacuo. Purification via flash column chromatography (eluent 30–40 °C petrol/Et_2O, 50:1) gave **10** as a colourless oil (45.1 g, 65% over three steps); R_f 0.64 (30–40 °C petrol/Et_2O, 10:1); δ_H (400 MHz, $CDCl_3$) 1.49 (9H, s, C*Me*$_3$), 1.90–1.98 (2H, m, C(4)*H*$_2$), 2.45–2.55 (4H, m, C(3)*H*$_2$, C(5)*H*$_2$), 6.67–6.68 (1H, m, C(2)*H*).

4.4. *tert*-Butyl (1*R*,2*S*,*S*)-2-[*N*-benzyl-*N*-(-methylbenzyl)amino]-cyclopentanecarboxylate 11

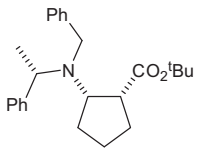

BuLi (2.5 M in hexanes, 28.4 mL, 71.0 mmol) was added dropwise to a solution of (*S*)-*N*-benzyl-*N*-(α-methylbenzyl)amine (15.5 g, 73.0 mmol) in THF (400 mL) at −78 °C. The resultant solution was allowed to stir at −78 °C for 30 min before the dropwise addition of a solution of **10** (7.70 g, 46.0 mmol) in THF (230 mL) at −78 °C. The reaction mixture was stirred at −78 °C for 3 h before the addition of satd aq NH_4Cl (50 mL). The reaction mixture was allowed to warm to rt before being concentrated in vacuo. The residue was dissolved in CH_2Cl_2 (100 mL), washed sequentially with 10% aq citric acid (100 mL), satd aq $NaHCO_3$ (100 mL) and brine (100 mL), then dried and concentrated in vacuo to give a 96:4 mixture of **11**:**12** as a colourless oil that solidified upon standing to a white crystalline solid (24.6 g, 87%).[12a] Recrystallisation of an aliquot from MeOH gave **11** as colourless crystals (>99:1 dr); mp 53–55 °C; $[\alpha]_D^{22} = -69.9$ (c 0.6 in $CHCl_3$); {lit.[12a] $[\alpha]_D^{25} = -69.1$ (c 1.2 in $CHCl_3$)}; δ_H (400 MHz, $CDCl_3$) 1.38–1.85 (6H, m, C(3)*H*$_2$, C(4)*H*$_2$, C(5)*H*$_2$) overlapping 1.38 (3H, d, J 6.9, C(α)*Me*) and 1.51 (9H, s, C*Me*$_3$), 2.89–2.93 (1H, m, C(1)*H*), 3.09–3.15 (1H, m, C(2)*H*), 3.54 (1H, d, J 15.5, NC*H*$_A$), 4.03 (1H, d, J 15.5, NC*H*$_B$), 4.31 (1H, q, J 6.9, C(α)*H*), 7.17–7.43 (10H, m, *Ph*).

4.4.1. X-ray crystal structure determination for 11

Data were collected using an Enraf-Nonius κ-CCD diffractometer with graphite monochromated Mo Kα radiation using standard procedures at 190 K. The structure was solved by direct methods (SIR92); all non-hydrogen atoms were refined with anisotropic thermal parameters. Hydrogen atoms were added at idealised positions. The structure was refined using CRYSTALS.[26]

X-ray crystal structure data for **11** [$C_{25}H_{33}NO_2$]: M = 379.54, monoclinic, space group $P2_1$, a = 10.0500(5) Å, b = 9.2191(4) Å, c = 12.1262(7) Å, β = 90.9075(17)°, V = 1112.36(10) Å^3, Z = 2, μ = 0.071 mm^{-1}, colourless plate, crystal dimensions = 0.20 × 0.30 × 0.40 mm^3. A total of 2694 unique reflections were measured for $5 < \theta < 27$ and 1589 reflections were used in the refinement. The final parameters were wR_2 = 0.072 and R_1 = 0.074 [$I > 2.5\sigma(I)$].

Crystallographic data (excluding structure factors) have been deposited with the Cambridge Crystallographic Data Centre as supplementary publication number CCDC 772467. Copies of the data can be obtained, free of charge, on application to CCDC, 12 Union Road, Cambridge CB2 1EZ, UK [fax: +44(0) 1223 336033 or e-mail: deposit@ccdc.cam.ac.uk].

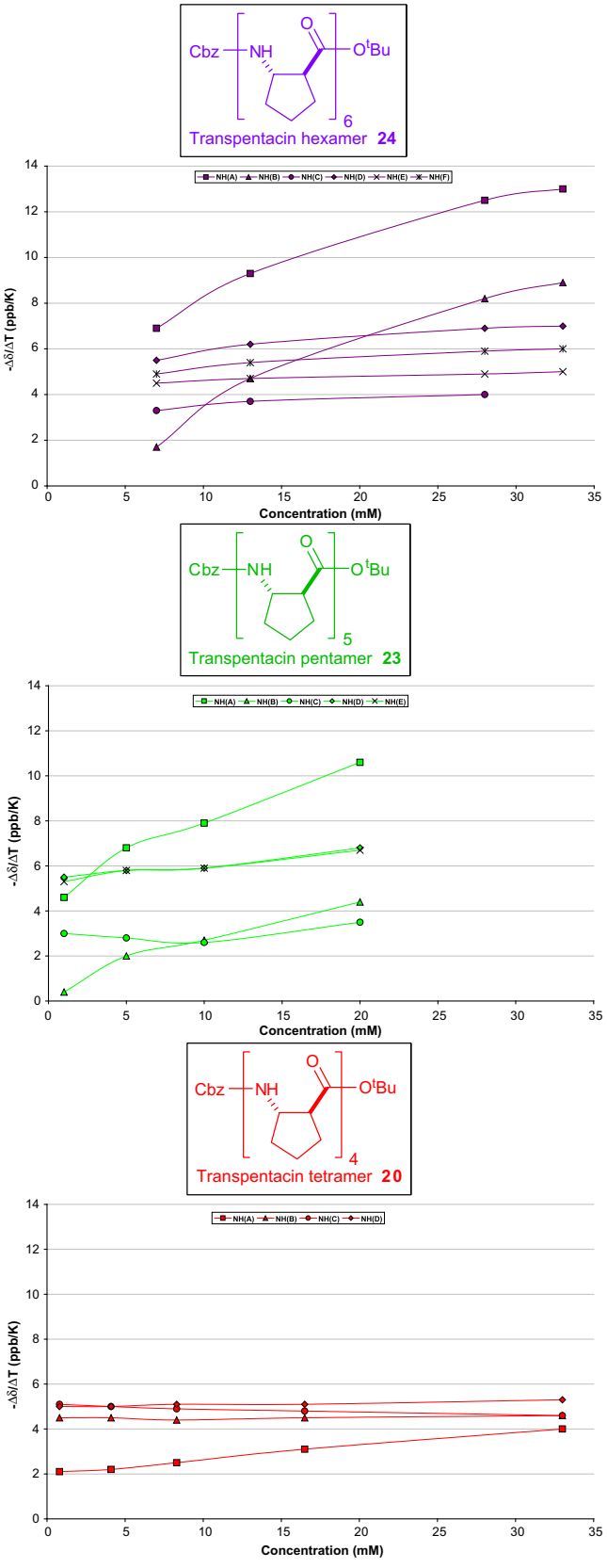

Figure 15. Temperature coefficients of amide protons within hexamer **24**, pentamer **23** and tetramer **20** over a range of concentrations.

4.5. *tert*-Butyl (*S,S,S*)-2-[*N*-benzyl-*N*-(-methylbenzyl)amino]cyclopentanecarboxylate 12

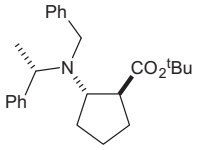

KO^{t}Bu (40% w/w substrate, 3.52 g) was added to a stirred solution of **11** (8.80 g, 23.2 mmol, 96:4 dr) in ^{t}BuOH (200 mL) and the resultant mixture was heated at reflux for 8 h. The reaction mixture was then allowed to cool to rt prior to the addition of satd aq NH_4Cl (200 mL). The resultant mixture was diluted with Et_2O (500 mL), the layers were separated and the organic layer was washed with brine (500 mL), dried and concentrated in vacuo to give a 96:4 mixture of **12** and (*S,S,S*)-2-[*N*-benzyl-*N*-(α-methylbenzyl)amino]cyclopentanecarboxylic acid. Purification via flash column chromatography (eluent 30–40 °C petrol/Et_2O, 20:1) gave **12** as a colourless oil that solidified upon standing to a white crystalline solid (7.1 g, 81%, >99:1 dr);[12a] R_f 0.48 (30–40 °C petrol/Et_2O, 10:1); mp 51–52 °C (MeOH); $[\alpha]_D^{20} = +62.4$ (*c* 1.0 in $CHCl_3$); {lit.[12a] $[\alpha]_D^{25} = +64.5$ (*c* 1.2 in $CHCl_3$)}; δ_H (400 MHz, $CDCl_3$) 1.33 (3H, d, *J* 6.8, C(α)*Me*), 1.39 (9H, s, C*Me*$_3$), 1.57–1.70 (4H, m, C(3)H_A, C(4)H_2, C(5)H_A), 1.74–1.81 (2H, m, C(3)H_B, C(5)H_B), 2.61–2.66 (1H, m, C(1)*H*), 3.55–3.63 (1H, m, C(2)*H*), 3.69 (1H, d, *J* 14.8, NCH_A), 3.78 (1H, d, *J* 14.8, NCH_B), 3.90 (1H, q, *J* 6.8, C(α)*H*), 7.14–7.46 (10H, m, *Ph*). Further elution (eluent 30–40 °C petrol/EtOAc, 2:1) gave (*S,S,S*)-2-[*N*-benzyl-*N*-(α-methylbenzyl)amino]cyclopentanecarboxylic acid as a white solid (94 mg, 1%, >99:1 dr); mp 130–134 °C; $[\alpha]_D^{21} = +58.9$ (*c* 1.2 in $CHCl_3$); ν_{max} (KBr) 1696 (C=O); δ_H (400 MHz, $CDCl_3$); 1.54 (3H, d, *J* 6.8, C(α)*Me*), 1.58–2.05 (6H, m, C(3)H_2, C(4)H_2, C(5)H_2), 2.79–2.90 (1H, m, C(1)*H*), 3.67 (1H, app q, *J* 9.1, C(2)*H*), 4.01 (1H, d, *J* 14.1, NCH_A), 4.23 (1H, d, *J* 14.1, NCH_B), 4.29 (1H, q, *J* 6.8, C(α)*H*), 7.13–7.59 (10H, m, *Ph*); δ_C (100 MHz, $CDCl_3$) 14.1 (C(α)*Me*), 22.5, 27.0, 27.0 (*C*(3), *C*(4), *C*(5)), 46.8 (*C*(1)), 50.3 (NCH_2), 60.1 (*C*(α)), 64.5 (*C*(2)), 128.3, 128.4, 128.6, 128.7, 128.9, 129.4 (*o,m,p-Ph*), 139.5, 136.6 (*i-Ph*), 178.3 (CO_2H); *m/z* (ESI$^+$) 382 ([M+MeCN+NH$_4$]$^+$, 28%), 346 ([M+Na]$^+$, 11%), 324 ([M+H]$^+$, 100%); HRMS (ESI$^+$) $C_{21}H_{26}NO_2^+$ ([M+H]$^+$) requires 324.1964; found 324.1966.

4.5.1. X-ray crystal structure determination for 12

Data were collected using an Enraf-Nonius κ-CCD diffractometer with graphite monochromated Mo Kα radiation using standard procedures at 190 K. The structure was solved by direct methods (SIR92); all non-hydrogen atoms were refined with anisotropic thermal parameters. Hydrogen atoms were added at idealised positions. The structure was refined using CRYSTALS.[26]

X-ray crystal structure data for **12** [$C_{25}H_{33}NO_2$]: $M = 379.54$, orthorhombic, space group $P2_12_12_1$, $a = 6.09210(10)$ Å, $b = 13.0837(2)$ Å, $c = 27.7214(6)$ Å, $V = 2209.60(7)$ Å^3, $Z = 4$, $\mu = 0.71$ mm^{-1}, colourless plate, crystal dimensions = 0.1 × 0.2 × 0.3 mm^3. A total of 2855 unique reflections were measured for $5 < \theta < 27$ and 2232 reflections were used in the refinement. The final parameters were $wR_2 = 0.039$ and $R_1 = 0.037$ [$I > 3\sigma(I)$].

Crystallographic data (excluding structure factors) have been deposited with the Cambridge Crystallographic Data Centre as supplementary publication number CCDC 772468. Copies of the data can be obtained, free of charge, on application to CCDC, 12 Union Road, Cambridge CB2 1EZ, UK [fax: +44(0) 1223 336033 or e-mail: deposit@ccdc.cam.ac.uk].

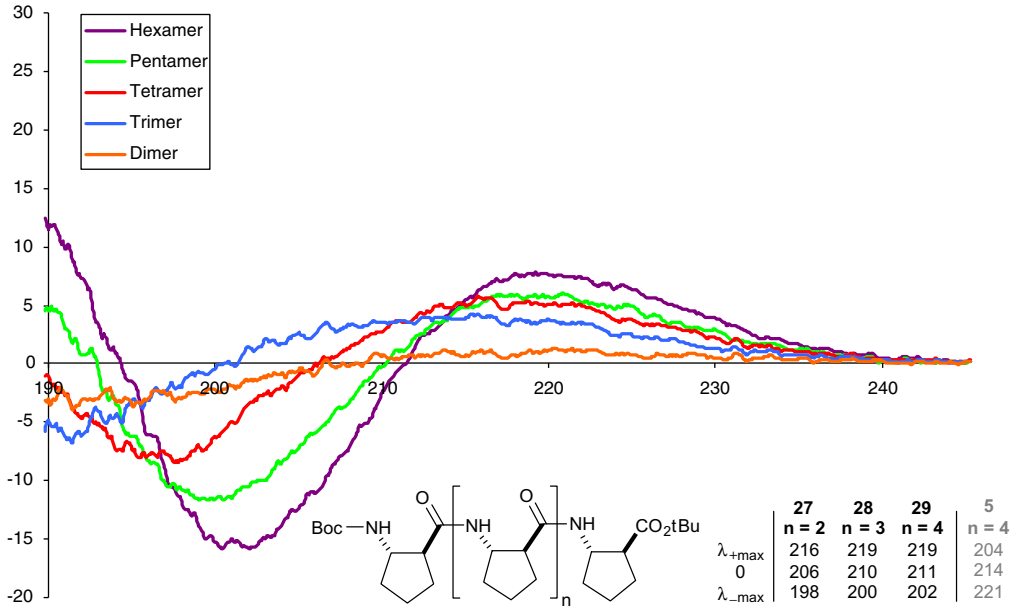

Figure 16. CD spectra of *N*-Boc dimer **25**, trimer **26**, tetramer **27**, pentamer **28** and hexamer **29** (1 mg/mL in TFE).

4.6. *tert*-Butyl (*S,S*)-2-aminocyclopentanecarboxylate 13

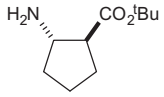

Following General Procedure 1, **12** (6.8 g, 17.8 mmol) and $Pd(OH)_2/C$ (25% w/w substrate, 1.70 g) in MeOH (80 mL) under H_2 (5 atm) gave **13** as a colourless oil that solidified upon standing to an off white solid (3.05 g, 92%, >99:1 dr); mp 84–86 °C; $[\alpha]_D^{23} = +59.4$ (*c* 1.1 in $CHCl_3$); ν_{max} (KBr) 3433 (N–H), 1725 (C=O); δ_H (400 MHz, $CDCl_3$, 26 mM) 1.30–1.42 (1H, m, C(3)H_A), 1.46 (9H, s, CMe_3), 1.55 (2H, s, NH_2), 1.66–1.70 (2H, m, C(4)H_2), 1.79–1.83 (1H, m, C(5)H_A), 1.91–2.05 (2H, m, C(3)H_B, C(5)H_B), 2.27–2.35 (1H, m, C(1)*H*), 3.34–3.42 (1H, m, C(2)*H*); δ_C (100 MHz, $CDCl_3$) 22.4 (*C*(4)), 27.9 (*C*(5)), 28.0 (CMe_3), 35.1 (*C*(3)), 54.5 (*C*(1)), 57.0 (*C*(2)), 79.9 (CMe_3), 174.5 (CO_2tBu); *m/z* (ESI$^+$) 186 ($[M+H]^+$ 100%); HRMS (ESI$^+$) $C_{10}H_{20}NO_2^+$ ($[M+H]^+$) requires 186.1494; found 186.1489.

4.7. *tert*-Butyl (*S,S*)-2-[*N*-(benzyloxycarbonyl)amino]cyclopentanecarboxylate 14

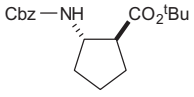

Et_3N (8.31 mL, 0.06 mol) and CbzCl (8.51 mL, 0.06 mol) were added successively to a stirred solution of **13** (9.20 g, 0.05 mol) in THF (100 mL) at 0 °C. The resultant mixture was then allowed to warm to rt and stirred for 16 h before the addition of brine (100 mL). The layers were separated and the aqueous layer was extracted with CH_2Cl_2 (2 × 100 mL). The combined organic layers were then dried and concentrated in vacuo. Purification via flash column chromatography (eluent 30–40 °C petrol/Et_2O, 7:1) gave **14** as a colourless oil (12.2 g, 77%, >99:1 dr); $C_{18}H_{25}NO_4$ requires C, 67.7; H, 7.9; N, 4.4; found C, 67.5; H, 7.9; N, 4.3; R_f 0.64 (30–40 °C petrol/Et_2O, 1:1); $[\alpha]_D^{23} = +34.9$ (*c* 1.0 in $CHCl_3$); ν_{max} (film) 3366 (N–H), 1725, 1704 (C=O); δ_H (400 MHz, $CDCl_3$, 26 mM) 1.36–1.54 (1H, m, C(3)H_A) overlapping 1.43 (9H, s, CMe_3), 1.65–1.76 (2H, m, C(4)H_2), 1.83–1.89 (1H, m, C(5)H_A), 1.92–1.97 (1H, m, C(5)H_B), 2.08–2.20 (1H, m, C(3)H_B), 2.46–2.54 (1H, m, C(1)*H*), 4.12–4.21 (1H, m, C(2)*H*), 4.81 (1H, br s, N*H*), 5.10 (2H, app s, CH_2Ph), 7.29–7.39 (5H, m, *Ph*); δ_C (125 MHz, $CDCl_3$) 22.7 (*C*(4)), 27.9 (*C*(5), CMe_3), 33.1 (*C*(3)), 51.6 (*C*(1)), 56.1 (*C*(2)), 66.5 (CH_2Ph), 80.4 (CMe_3), 127.9, 128.4, 128.5 (*o,m,p-Ph*), 136.4 (*i-Ph*), 155.5 (NCO), 173.5 (CO_2tBu); *m/z* (ESI$^+$) 378 ($[M+MeCN+NH_4]^+$, 100%); HRMS (ESI$^+$) $C_{18}H_{25}NNaO_4^+$ ($[M+Na]^+$) requires 342.1681; found 342.1679.

4.8. (*S,S*)-2-[*N*-(Benzyloxycarbonyl)amino]cyclopentanecarboxylic acid 15

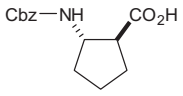

Following General Procedure 2, **14** (5.90 g, 0.02 mol) and TFA (12 mL) in CH_2Cl_2 (48 mL) gave, after purification via recrystallisation ($CHCl_3$/heptane), **15** as a white crystalline solid (4.23 g, 87%, >99:1 dr); $C_{14}H_{17}NO_4$ requires C, 63.9; H, 6.5; N, 5.3; found C, 64.1; H, 6.5; N, 5.2; mp 100–101 °C ($CHCl_3$/heptane); $[\alpha]_D^{18} = +23.5$ (*c* 1.3 in $CHCl_3$); ν_{max} (film) 3323 (O–H), 1706, 1704 (C=O); δ_H (400 MHz, $CDCl_3$, 26 mM) 1.42–1.55 (1H, m, C(3)H_A), 1.66–1.79 (2H, m, C(4)H_2), 1.86–2.00 (1H, m, C(5)H_A), 2.07–2.21 (2H, m, C(3)H_B, C(5)H_B), 2.73–2.85 (1H, m, C(1)*H*), 4.06–4.20 (1H, m, C(2)*H*), 5.08 (1H, s, N*H*), 5.14 (2H, s, CH_2Ph), 7.31–7.44 (5H, m, *Ph*); δ_C (125 MHz, CD_3OD) 23.2 (*C*(4)), 28.9 (*C*(5)), 32.8 (*C*(3)), 50.6 (*C*(1)), 56.3 (*C*(2)), 66.3 (CH_2Ph), 127.8, 127.9, 128.4 (*o,m,p-Ph*), 137.4 (*i-Ph*), 157.4 (NCO), 176.2 (CO_2H); *m/z* (ESI$^+$) 322 ($[M+MeCN+NH_4]^+$, 100%), 286 ($[M+Na]^+$, 95%); HRMS (ESI$^+$) $C_{14}H_{17}NNaO_4^+$ ($[M+Na]^+$) requires 286.1055; found 286.1056.

4.8.1. X-ray crystal structure determination for 15

Data were collected using an Enraf-Nonius κ-CCD diffractometer with graphite monochromated Mo Kα radiation using standard procedures at 190 K. The structure was solved by direct methods (SIR92); all non-hydrogen atoms were refined with anisotropic thermal parameters. Hydrogen atoms were added at idealised positions. The structure was refined using CRYSTALS.[26]

X-ray crystal structure data for **15** [$C_{14}H_{17}NO_4$]: M = 263.29, monoclinic, space group $P2_1$, a = 15.9879(8) Å, b = 4.9448(3) Å, c = 18.8621(13) Å, β = 112.521(2), V = 1377.46(15) Å^3, Z = 4, μ = 0.093 mm^{-1}, colourless plate, crystal dimensions = 0.1 × 0.1 × 0.3 mm^3. A total of 3027 unique reflections were measured for $5 < \theta < 27$ and 2261 reflections were used in the refinement. The final parameters were wR_2 = 0.110 and R_1 = 0.058 [$I > 2.0\sigma(I)$]. Crystallographic data (excluding structure factors) have been deposited with the Cambridge Crystallographic Data Centre as supplementary publication number CCDC 772469. Copies of the data can be obtained, free of charge, on application to CCDC, 12 Union Road, Cambridge CB2 1EZ, UK [fax: +44(0) 1223 336033 or e-mail: deposit@ccdc.cam.ac.uk].

4.9. Cbz-[(*S*,*S*)-ACPC]$_2$-O^{t}Bu 16

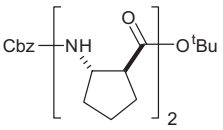

Following General Procedure 3 **15** (4.20 g, 16.0 mmol), **13** (2.95 g, 16.0 mmol), HOBt (2.59 g, 19.0 mmol), EDC·HCl (3.67 g, 19.0 mmol) and Et_3N (11.1 mL, 80.0 mol) in $CHCl_3$ (10 mL) gave, after purification via recrystallisation ($CHCl_3$/heptane), **16** as a white solid (5.30 g, 77%, >99:1 dr); $C_{24}H_{34}N_2O_5$ requires C, 66.95; H, 8.0; N, 6.5; found C, 66.8; H, 8.0; N, 6.5; mp 142–144 °C ($CHCl_3$/heptane); $[\alpha]_D^{23} = +39.0$ (c 1.1 in $CHCl_3$); ν_{max} (film) 3324 (N–H), 1720, 1689, 1645, 1539 (C=O); δ_H (400 MHz, $CDCl_3$, 26 mM) 1.37–1.55 (2H, m, 2 × C(3)H_A) overlapping 1.44 (9H, s, CMe_3), 1.60–1.77 (4H, m, 2 × C(4)H_2), 1.81–1.88 (2H, m, 2 × C(5)H_A), 2.01–2.06 (4H, m, 2 × C(3)H_B, 2 × C(5)H_B), 2.52–2.62 (1H, m, C(1)*H*), 2.63–2.67 (1H, m, C(1)*H*), 3.97–4.07 (1H, m, C(2)*H*), 4.33–4.45 (1H, m, C(2)*H*), 4.92 (1H, d, *J* 4.6, N*H*), 5.12 (2H, s, CH_2Ph), 7.32–7.41 (6H, m, N*H*, *Ph*); δ_C (100 MHz, $CDCl_3$) 23.1, 24.3 (2 × *C*(4)), 27.3, 28.2 (2 × *C*(5)), 28.0 (CMe_3), 32.9, 33.3 (2 × *C*(3)), 51.7, 52.8 (2 × *C*(1)), 54.5, 57.1 (2 × *C*(2)), 66.9 (CH_2Ph), 80.2 (*C*Me$_3$), 128.1, 128.3, 128.6 (*o*,*m*,*p*-*Ph*), 136.2 (*i*-*Ph*), 156.7, 174.1, 175.5 (C=O); m/z (ESI$^+$) 489 ([M+MeCN+NH$_4$]$^+$, 100%); HRMS (ESI$^+$) $C_{24}H_{34}N_2NaO_5^+$ ([M+Na]$^+$) requires 453.2365; found 453.2360.

4.10. H-[(*S*,*S*)-ACPC]$_2$-O^{t}Bu 17

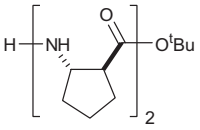

Following General Procedure 1, **16** (1.96 g, 4.60 mmol) and Pd(OH)$_2$/C (25% w/w substrate, 490 mg) in MeOH (20 mL) under H_2 (1 atm) gave **17** as a white solid (1.31 g, 97%, >99:1 dr); mp 101–103 °C; $[\alpha]_D^{23} = +50.1$ (c 0.8 in $CHCl_3$); ν_{max} (film) 3290 (N–H), 1723, 1646 (C=O); δ_H (400 MHz, $CDCl_3$, 26 mM) 1.22–1.52 (2H, m, 2 × C(3)H_A) overlapping 1.45 (9H, s, CMe_3), 1.57–1.81 (6H, m, 2 × C(4)H_2, NH_2), 1.82–2.21 (7H, m, C(1)*H*, 2 × C(3)H_B, 2 × C(5)H_2), 2.45–2.53 (1H, m, C(1)*H*), 3.16–3.25 (1H, m, C(2)*H*), 4.34–4.43 (1H, m, C(2)*H*), 7.03 (1H, d, *J* 7.6 N*H*); δ_C (100 MHz, $CDCl_3$) 21.8, 22.8 (2 × *C*(4)), 26.6, 27.9 (2 × *C*(5)), 28.0 (CMe_3), 32.9, 36.7 (2 × *C*(3)), 52.1, 52.9 (2 × *C*(1)), 54.4, 57.4 (2 × *C*(2)), 80.5 (*C*Me$_3$), 173.8, 175.5 (C=O); m/z (ESI$^+$) 355 ([M+MeCN+NH$_4$]$^+$, 100%), 297 ([M+H]$^+$, 95%); HRMS (ESI$^+$) $C_{16}H_{29}N_2O_3^+$ ([M+H]$^+$) requires 297.2178; found 297.2180.

4.11. Cbz-[(*S*,*S*)-ACPC]$_2$-OH 18

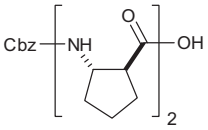

Following General Procedure 2, **16** (2.50 g, 5.80 mmol) and TFA (7 mL) in CH_2Cl_2 (21 mL) gave a colourless oil. Addition of Et_2O (40 mL) resulted in the formation of a white powder that was collected by suction filtration to give **18** as a white solid (1.87 mg, 86%, >99:1 dr); $C_{20}H_{26}N_2O_5$ requires C, 64.15; H, 7.0; N, 7.5; found C, 64.0; H, 7.0; N, 7.4; mp 144–146 °C; $[\alpha]_D^{18} = +28.6$ (c 1.6 in $CHCl_3$); ν_{max} (film) 3302 (O–H), 1694, 1554 (C=O); δ_H (400 MHz, $CDCl_3$, 26 mM) 1.42–1.55 (1H, m, C(3)H_A), 1.60–2.17 (10H, m, C(3)H_A, 2 × C(3)H_B, 2 × C(4)H_2, 2 × C(5)H_A, C(5)H_B), 2.18–2.30 (1H, m, C(5)H_B), 2.68–2.72 (1H, m, C(1)*H*), 2.75–2.79 (1H, m, C(1)*H*), 3.97–4.03 (1H, m, C(2)*H*), 4.04–4.09 (1H, m, C(2)*H*), 5.03 (1H, d, *J* 6.1, N*H*), 5.11 (2H, app s, CH_2Ph), 7.31–7.43 (5H, m, *Ph*), 8.25 (1H, br s, N*H*); δ_C (100 MHz, CD_3OD) 22.8, 23.4 (2 × *C*(4)), 28.6, 29.4 (2 × *C*(5)), 32.0, 38.4 (2 × *C*(3)), 48.4, 50.0 (2 × *C*(1)), 54.4, 57.4 (2 × *C*(2)), 66.1 (*C*H$_2$Ph), 127.2, 127.4, 127.6, 128.1, 129.1 (*o*,*m*,*p*-*Ph*), 137.7 (*i*-*Ph*), 157.0, 175.7 (C=O); m/z (ESI$^+$) 433 ([M+MeCN+NH$_4$]$^+$, 100%), 375 ([M+H]$^+$, 95%); HRMS (ESI$^+$) $C_{20}H_{27}N_2O_5^+$ ([M+H]$^+$) requires 375.1920; found 375.1913.

4.11.1. X-ray crystal structure determination for 18

Data were collected using an Enraf-Nonius κ-CCD diffractometer with graphite monochromated Mo Kα radiation using standard procedures at 190 K. The structure was solved by direct methods (SIR92); all non-hydrogen atoms were refined with anisotropic thermal parameters. Hydrogen atoms were added at idealised positions. The structure was refined using CRYSTALS.[26]

X-ray crystal structure data for **18** [$C_{20}H_{26}N_2O_5$]: M = 374.44, triclinic, space group $P1$, a = 5.9632(2) Å, b = 8.8669(3) Å, c = 10.0968(4) Å, α = 76.807(2)°, β = 82.639(2)°, γ = 75.7607(14)°, V = 502.34(3) Å^3, Z = 1, μ = 0.089 mm^{-1}, colourless plate, crystal dimensions = 0.1 × 0.1 × 0.2 mm^3. A total of 2226 unique reflections were measured for $5 < \theta < 27$ and 1526 reflections were used in the refinement. The final parameters were wR_2 = 0.052 and R_1 = 0.046 [$I > 1.5\sigma(I)$].

Crystallographic data (excluding structure factors) have been deposited with the Cambridge Crystallographic Data Centre as supplementary publication number CCDC 772470. Copies of the data can be obtained, free of charge, on application to CCDC, 12 Union Road, Cambridge CB2 1EZ, UK [fax: +44(0) 1223 336033 or e-mail: deposit@ccdc.cam.ac.uk].

4.12. Cbz-[(*S*,*S*)-ACPC]$_3$-O^{t}Bu 19

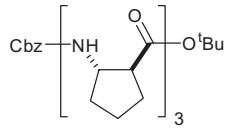

Following General Procedure 3, **15** (874 mg, 3.32 mmol), **17** (984 mg, 3.32 mmol), HOBt (538 mg, 3.98 mmol), EDC·HCl (764 mg, 3.98 mmol) and Et_3N (2.31 mL, 16.6 mmol) in $CHCl_3$ (10 mL) gave, after purification via recrystallisation ($CHCl_3$/heptane), **19** as a white solid (1.29 mg, 72%, >99:1 dr); mp 193–195 °C ($CHCl_3$/heptane); $[\alpha]_D^{23} = +46.6$ (c 1.0 in $CHCl_3$); ν_{max} (KBr) 3319 (N–H), 1719, 1684, 1644, 1539 (C=O); δ_H (400 MHz, $CDCl_3$, 26 mM) 1.38–1.61 (3H, m, 3 × C(3)H_A) overlapping 1.43 (9H, s, CMe_3), 1.65–1.77 (6H, m, 3 × C(4)H_2), 1.90–2.12 (9H, m, 3 ×

C(3)H$_A$H$_B$, 3 × C(5)H_2), 2.43–2.64 (1H, C(1)H), 2.65–2.68 (2H, m, 2 × C(1)H), 3.96–4.05 (1H, m, C(2)H), 4.15 (1H, app t, J 6.1, C(2)H), 4.35–4.46 (1H, m, C(2)H), 5.00 (1H, d, J 6.5, NH), 5.10 (2H, s, CH_2Ph), 7.30–7.41 (5H, m, Ph), 7.45 (1H, d, J 6.1, NH), 7.93 (1H, d, J 7.9, NH); δ_C (100 MHz, $CDCl_3$) 23.2, 24.0, 24.4, 27.3, 27.6, 28.4, 32.9, 33.0, 33.6 (3 × C(3), 3 × C(4), 3 × C(5)), 28.0 (CMe_3), 51.7, 53.0, 53.2 (3 × C(1)), 54.5, 55.8, 56.9 (3 × C(2)), 67.1 (CH_2Ph), 80.1 (CMe$_3$), 128.1, 128.3, 128.6 (*o*,*m*,*p*-*Ph*), 136.1 (*i*-*Ph*), 156.8 (NCO [carbamate]), 173.1, 174.2, 174.3 (2 × NCO [amide], CO_2^{t}Bu); m/z (ESI$^+$) 564 ([M+Na]$^+$, 41%), 542 ([M+H]$^+$, 32%), 486 ([M−C$_4$H$_9$]$^+$, 100%); HRMS (ESI$^+$) $C_{30}H_{43}N_3NaO_6^+$ ([M+Na]$^+$) requires 564.3044; found 564.3045.

4.13. Cbz-[(*S*,*S*)-ACPC]$_4$-O^{t}Bu 20

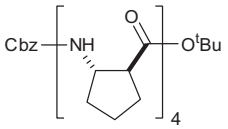

Following General Procedure 3, **18** (500 mg, 1.34 mmol), **17** (396 mg, 1.34 mmol), HOBt (217 mg, 1.60 mmol), EDC·HCl (307 mg, 1.60 mmol) and Et$_3$N (0.93 mL, 6.68 mmol) in $CHCl_3$ (7 mL) gave, after purification via recrystallisation ($CHCl_3$/heptane), **20** as a white solid (632 mg, 73%, >99:1 dr); $C_{36}H_{52}N_4O_7$ requires C, 66.2; H, 8.0; N, 8.6; found C, 65.9; H, 7.9; N 8.5; mp 224–226 °C ($CHCl_3$/heptane); $[\alpha]_D^{23} = +45.2$ (c 0.6 in $CHCl_3$); ν_{max}/cm^{-1} (film) 3330 (br, NH), 1720, 1703, 1647, 1553 (C=O); δ_H (400 MHz, $CDCl_3$, 26 mM) 1.35–1.53 (4H, m, 4 × C(3)H_A) overlapping 1.43 (9H, s, CMe_3), 1.65–1.98 (20H, m, 4 × C(3)$_A$H$_B$, 4 × C(4)H_2, 4 × C(5)H_2), 2.31–2.40 (1H, m, C(1)H), 2.45–2.52 (1H, m, C(1)H), 2.55–2.61 (1H, m, C(1)H), 2.64–2.70 (1H, m, C(1)H), 4.01 (1H, app qt, J 6.8, C(2)H), 4.14–4.26 (2H, m, 2 × C(2)H), 4.36–4.46 (1H, m, C(2)H), 5.09 (2H, s, CH_2Ph), 5.18 (1H, d, J 6.5, NH), 7.08 (1H, d, J 6.8, NH), 7.30–7.41 (5H, m, Ph), 7.86 (1H, d, J 6.5, NH), 8.10 (1H, d, J 7.5, NH); δ_C (125 MHz, $CDCl_3$) 22.2, 23.0, 23.3, 23.5 (4 × C(4)), 26.2, 26.5, 26.9, 27.0, 27.5 (4 × C(5), CMe_3), 31.8, 31.9, 32.2, 32.3 (4 × C(3)), 49.0, 51.5, 51.8, 52.0 (4 × C(1)), 52.3, 53.4, 54.5, 56.1 (4 × C(2)), 66.1 (CH_2Ph), 79.0 (CMe$_3$), 127.1, 127.2, 127.3, 127.4, 127.6 (*o*,*m*,*p*-*Ph*), 135.0 (*i*-*Ph*), 155.7, 172.3, 173.3, 173.4, 173.5 (C=O); m/z (ESI$^+$) 711 ([M+MeCN+NH$_4$]$^+$, 100%), 675 ([M+Na]$^+$, 50%), 653 ([M+H]$^+$, 20%); HRMS (ESI$^+$) $C_{36}H_{53}N_4O_7^+$ ([M+H]$^+$) requires 653.3914; found 653.3915.

4.14. H-[(*S*,*S*)-ACPC]$_3$-O^{t}Bu 21

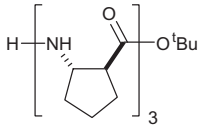

Following General Procedure 1, **19** (405 mg, 0.75 mmol) and Pd(OH)$_2$/C (25% w/w substrate, 101 mg) in MeOH (10 mL) under H_2 (1 atm) gave **21** as a white solid (272 mg, 89%, >99:1 dr); mp 198–200 °C (dec); $[\alpha]_D^{23} = +46.4$ (c 0.9 in $CHCl_3$); ν_{max} (KBr) 3264 (N–H), 1725, 1634 (C=O); δ_H (400 MHz, $CDCl_3$, 26 mM) 1.24–1.78 (11H, m, 3 × C(3)H_A, 3 × C(4)H_2, NH_2) overlapping 1.43 (9H, s, CMe_3), 1.79–2.26 (10H, m, C(1)H, 3 × C(3)H_B, 3 × C(5)H_2), 2.50–2.67 (2H, m, 2 × C(1)H), 3.07–3.17 (1H, m, C(2)H), 4.12–4.21 (1H, m, C(2)H), 4.35–4.45 (1H, m, C(2)H), 7.68 (1H, d, J 6.3, NH), 8.14 (1H, d, J 7.6, NH); δ_C (100 MHz, $CDCl_3$) 21.5, 23.2, 24.3, 26.2, 27.3, 28.3, 33.0, 33.1, 37.5 (3 × C(3), 3 × C(4), 3 × C(5)), 28.0 (CMe_3), 51.7, 52.0, 53.5 (3 × C(1)), 54.5, 55.3, 57.4 (3 × C(2)), 80.1 (CMe$_3$), 172.9, 174.3, 175.5 (2 × NCO, CO_2^{t}Bu); m/z (ESI$^+$) 430 ([M+Na]$^+$, 95%), 352 ([M−C$_4$H$_9$]$^+$, 100%); HRMS (ESI$^+$) $C_{22}H_{38}N_3O_4^+$ ([M+H]$^+$) requires 408.2857; found 408.2857.

4.15. H-[(*S*,*S*)-ACPC]$_4$-O^{t}Bu 22

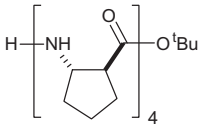

Following General Procedure 1, **20** (158 mg, 0.24 mmol) and Pd(OH)$_2$/C (50% w/w substrate, 79.2 mg) in MeOH (5 mL) under H_2 (1 atm) gave **22** as a white solid (112 mg, 89%, >99:1 dr); mp 201–203 °C (dec); $[\alpha]_D^{23} = +59.7$ (c 0.6 in $CHCl_3$); ν_{max} (KBr) 3307 (N–H), 1722, 1653 (C=O); δ_H (400 MHz, $CDCl_3$, 26 mM) 1.29–2.27 (27H, m, C(1)H, 4 × C(3)H_2, 4 × C(4)H_2, 4 × C(5)H_2, NH_2) overlapping 1.42 (9H, s, CMe_3), 2.51–2.65 (3H, m, 3 × C(1)H), 3.08–3.18 (1H, m, C(2)H), 4.08–4.21 (2H, m, 2 × C(2)H), 4.36–4.46 (1H, m, C(2)H), 7.80 (1H, d, J 6.8, NH), 8.05 (1H, d, J 7.9, NH), 8.35 (1H, d, J 6.5, NH); δ_C (100 MHz, $CDCl_3$) 21.5, 23.3, 24.2, 24.2, 26.2, 27.5, 27.6, 28.4, 32.9, 32.9, 33.3, 37.5 (4 × C(3), 4 × C(4), 4 × C(5)), 28.0 (CMe_3), 51.7, 51.8, 53.1, 53.6 (4 × C(1)), 54.4, 55.1, 55.5, 57.4 (4 × C(2)), 80.1 (CMe$_3$), 173.2, 174.4, 175.6 (3 × NCO, CO_2^{t}Bu); m/z (ESI$^+$) 541 ([M+Na]$^+$, 42%), 519 ([M+H]$^+$, 23%), 463 ([M−C$_4$H$_8$]$^+$, 100%); HRMS (ESI$^+$) $C_{28}H_{47}N_4O_5^+$ ([M+H]$^+$) requires 519.3541; found 519.3545.

4.16. Cbz-[(*S*,*S*)-ACPC]$_5$-O^{t}Bu 23

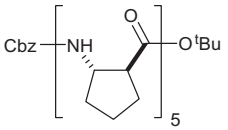

Following General Procedure 3, **18** (66.0 mg, 0.18 mmol), **21** (71.8 mg, 0.18 mmol), HOBt (28.6 mg, 0.21 mmol), EDC·HCl (40.5 mg, 0.21 mmol) and Et$_3$N (0.12 mL, 0.88 mmol) in $CHCl_3$ (3 mL) gave, after purification via recrystallisation ($CHCl_3$/heptane), **23** as a white solid (74.9 mg, 56%, >99:1 dr); mp 232–234 °C ($CHCl_3$/heptane); $[\alpha]_D^{23} = +53.8$ (c 0.3 in $CHCl_3$); ν_{max} (KBr) 3279 (N–H), 1716, 1698, 1640, 1563 (C=O); δ_H (400 MHz, $CDCl_3$, 14 mM) 1.20–2.23 (16H, m, C(1)H, 5 × C(3)H_2, 5 × C(4)H_2, 5 × C(5)H_2) overlapping 1.43 (1H, s, CMe_3), 2.31–2.52 (1H, m, C(1)H), 2.54–2.68 (2H, m, 2 × C(1)H), 2.70–2.83 (1H, m, C(1)H), 4.01–4.07 (1H, m, C(2)H), 4.20–4.26 (3H, m, 3 × C(2)H), 4.36–4.49 (1H, m, C(2)H), 5.07 (1H, d, J 12.3, CH_AH$_B$Ph), 5.13 (1H, d, J 12.3, CH$_A$$H_B$Ph), 5.28 (1H, d, J 7.5, NH), 6.49 (1H, d, J 7.9, NH), 7.22–7.43 (5H, m, Ph), 7.47 (1H, d, J 8.2, NH), 8.09 (1H, d, J 7.2, NH), 8.19 (1H, d, J 7.5, NH); δ_C (125 MHz, $CDCl_3$) 23.8, 24.4, 24.6, 24.8, 27.7, 28.2, 28.4, 28.5, 28.6, 32.7, 33.3, 33.5, 33.6, 33.7 (5 × C(3), 5 × C(4), 5 × C(5)), 28.0 (CMe_3), 51.3, 52.4, 52.6, 53.6, 53.6, 54.4, 55.3, 55.4, 57.3 (5 × C(1), 5 × C(2)), 67.0 (CH_2Ph), 79.9 (CMe$_3$), 127.8, 127.9, 128.4, 128.6 (*o*,*m*,*p*-*Ph*), 136.2 (*i*-*Ph*), 156.5 (NCO [carbamate]), 173.8, 174.1, 174.5, 174.8 (4 × NCO [amide], CO_2^{t}Bu); m/z (ESI$^+$) 786 ([M+Na]$^+$, 52%), 764 ([M+H]$^+$, 58%), 708 [(M−C$_4$H$_8$]$^+$, 100%); HRMS (ESI$^+$) $C_{42}H_{62}N_5O_8^+$ ([M+H]$^+$) requires 764.4593; found 764.4597.

4.17. Cbz-[(*S*,*S*)-ACPC]$_6$-O^{t}Bu 24

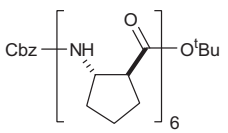

Following General Procedure 3, **18** (121 mg, 0.32 mmol), **22** (168 mg, 0.32 mmol), HOBt (52.5 mg, 0.39 mmol), EDC·HCl (74.5 mg, 0.39 mmol) and Et$_3$N (0.20 mL, 1.62 mmol) in $CHCl_3$

(40 mL) gave, after purification via flash column chromatography (eluent $CHCl_3$/MeOH, 20:1), **24** (187 mg, 66%, >99:1 dr) as a white solid; R_f 0.48 ($CHCl_3$/MeOH, 10:1); mp 185–187 °C; $[\alpha]_D^{20} = +49.2$ (*c* 0.2 in $CHCl_3$); ν_{max} (KBr) 3298 (N–H), 1723, 1704, 1648, 1556 (C=O); δ_H (400 MHz, $CDCl_3$, 7 mM) 1.31–2.20 (37H, m, C(1)*H*, 6 × C(3)H_2, 6 × C(4)H_2, 6 × C(5)H_2) overlapping 1.44 (9H, s, CMe_3), 2.29–2.36 (2H, m, 2 × C(1)*H*), 2.41–2.46 (1H, m, C(1)*H*), 2.62–2.71 (1H, m, C(1)*H*), 2.79–2.89 (1H, m, C(1)*H*), 3.91–3.98 (1H, m, C(2)*H*), 4.22–4.34 (4H, m, 4 × C(2)*H*), 4.38–4.48 (1H, m, C(2)*H*), 5.06 (1H, d, *J* 12.5, CH_AH_BPh), 5.50 (1H, d, *J* 12.5, CH_AH_BPh), 5.50 (1H, d, *J* 7.9, N*H*), 6.30 (1H, d, *J* 7.9, N*H*), 4.26–7.41 (6H, m, N*H*, *Ph*), 8.10 (1H, d, *J* 8.5, N*H*), 8.22 (1H, d, *J* 7.9, N*H*), 8.31 (1H, d, *J* 7.5, N*H*); δ_C (100 MHz, $CDCl_3$) 22.6, 23.8, 24.4, 24.7, 24.8, 25.2 (6 × *C*(4)), 27.2, 28.0, 28.1, 28.2, 28.3, 28.5, 29.0 (6 × *C*(5), CMe_3), 31.8, 32.3, 32.6, 33.0, 33.1, 33.3 (6 × *C*(3)), 50.5, 51.1, 51.2, 52.1, 52.2, 52.3 (6 × *C*(1)), 54.2, 54.3, 55.2, 55.3, 55.4, 56.0 (6 × *C*(2)), 66.6 (CH_2Ph), 79.9 (*C*Me$_3$), 127.7, 128.1, 128.5 (*o*,*m*,*p*-*Ph*), 136.6 (*i*-*Ph*), 156.7 (N*C*O [carbamate]), 173.3, 173.4, 173.5, 174.4, 174.6, 174.8 (5 × N*C*O [amide], $CO_2{}^tBu$); *m*/*z* (ESI^+) 933 ($[M+MeCN+NH_4]^+$, 100%), 897 ($[M+Na]^+$, 50%); HRMS (ESI^+) $C_{48}H_{71}N_6O_9{}^+$ ($[M+H]^+$) requires 875.5283; found 875.5313.

4.18. Boc-[(*S*,*S*)-ACPC]$_2$-O^{t}Bu 25

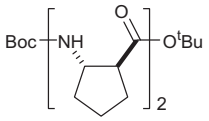

Following General Procedure 4, **16** (148 mg, 0.34 mmol), Boc_2O (82.4 mg, 0.38 mmol) and $Pd(OH)_2$/C (25% w/w substrate, 37 mg) in MeOH (10 mL) gave, after purification via trituration with Et_2O, **25** as a white crystalline solid (110 mg, 81%, >99:1 dr); $C_{21}H_{36}N_2O_5$ requires C, 63.6; H, 9.2; N, 7.1; found C, 63.7; H, 9.2; N, 7.0; mp 200–202 °C ($CHCl_3$/heptane); $[\alpha]_D^{18} = +33.1$ (*c* 0.7 in $CHCl_3$); ν_{max} (KBr) 3317 (N–H), 1718, 1684, 1652, 1558 (C=O); δ_H (400 MHz, $CDCl_3$, 26 mM) 1.35–1.57 (2H, m, 2 × C(3)H_A) overlapping 1.44 (9H, s, CMe_3) and 1.45 (9H, s, CMe_3), 1.63–1.78 (4H, m, 2 × C(4)H_2), 1.81–1.92 (2H, m, 2 × C(5)H_A), 1.94–2.14 (4H, m, 2 × C(3)H_B, 2 × C(5)H_B), 2.53–2.65 (2H, m, 2 × C(1)*H*), 3.91–4.00 (1H, m, C(2)*H*), 4.39 (1H, app qt, *J* 7.1 C(2)*H*), 4.67 (1H, d, *J* 6.1, N*H*), 7.69 (1H, br s, N*H*); δ_C (100 MHz, $CDCl_3$) 23.1, 24.1, 27.5, 28.3, 32.9, 33.5 (2 × *C*(3), 2 × *C*(4), 2 × *C*(5)), 28.0, 28.4 (2 × CMe_3), 51.6, 55.3 (2 × *C*(1)), 54.5, 56.3 (2 × *C*(2)), 80.0, 80.1 (2 × CMe_3), 156.4 (N*C*O [carbamate]), 172.9, 174.2 (2 × N*C*O [amide], $CO_2{}^tBu$); *m*/*z* (ESI^+) 419 ($[M+Na]^+$, 100%), 397 ($[M+H]^+$, 24%); HRMS (ESI^+) $C_{21}H_{36}N_2NaO_5{}^+$ ($[M+Na]^+$) requires 419.2516; found 419.2515.

4.18.1. X-ray crystal structure determination for 25

Data were collected using an Enraf-Nonius κ-CCD diffractometer with graphite monochromated Mo Kα radiation using standard procedures at 190 K. The structure was solved by direct methods (SIR92); all non-hydrogen atoms were refined with anisotropic thermal parameters. Hydrogen atoms were added at idealised positions. The structure was refined using CRYSTALS.[26]

X-ray crystal structure data for **25** [$C_{21}H_{36}N_2O_5$]: M = 396.53, orthorhombic, space group $P2_12_12_1$, a = 5.25520(10) Å, b = 18.6766(3) Å, c = 22.3554(4) Å, V = 2194.17(7) Å^3, Z = 4, μ = 0.085 mm^{-1}, colourless plate, crystal dimensions = 0.05 × 0.05 × 0.1 mm^3. A total of 2876 unique reflections were measured for $5 < \theta < 27$ and 1582 reflections were used in the refinement. The final parameters were wR_2 = 0.035 and R_1 = 0.030 [$I > 3.0\sigma(I)$].

Crystallographic data (excluding structure factors) have been deposited with the Cambridge Crystallographic Data Centre as supplementary publication number CCDC 772471. Copies of the data can be obtained, free of charge, on application to CCDC, 12 Union Road, Cambridge CB2 1EZ, UK [fax: +44(0) 1223 336033 or e-mail: deposit@ccdc.cam.ac.uk].

4.19. Boc-[(*S*,*S*)-ACPC]$_3$-O^{t}Bu 26

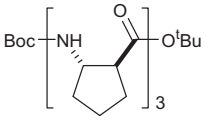

Following General Procedure 4, **19** (196 mg, 0.36 mmol), Boc_2O (86.7 mg, 0.40 mmol) and $Pd(OH)_2$/C (25% w/w substrate, 49 mg) in MeOH (10 mL) gave, after purification via recrystallisation ($CHCl_3$/heptane), **26** as a white solid (147 mg, 80%, >99:1 dr); mp 208–210 °C ($CHCl_3$/heptane); $[\alpha]_D^{23} = +36.2$ (*c* 0.5 in $CHCl_3$); ν_{max} (2 mM solution in $CHCl_3$) 3441, 3280 (N–H); ν_{max} (KBr) 3424 (N–H), 1717, 1646, 1559, 1541 (C=O); δ_H (400 MHz, $CDCl_3$, 26 mM) 1.36–1.62 (3H, m, 3 × C(3)H_A) overlapping 1.43 (9H, s, CMe_3) and 1.45 (9H, s, CMe_3), 1.65–1.80 (6H, m, 3 × C(4)H_2), 1.80–2.19 (9H, m, 3 × C(3)H_B, 3 × C(5)H_2), 2.52–2.67 (3H, m, 3 × C(1)*H*), 3.91–4.00 (1H, m, C(2)*H*), 4.12–4.20 (1H, m, C(2)*H*), 4.37–4.46 (1H, m, C(2)*H*), 4.71 (1H, d, *J* 7.1, N*H*), 4.80 (1H, d, *J* 5.6, N*H*), 8.03 (1H, d, *J* 7.6, N*H*); δ_C (100 MHz, $CDCl_3$) 23.2, 23.9, 24.4, 27.3, 27.8, 33.0, 33.7 (3 × *C*(3), 3 × *C*(4), 3 × *C*(5)), 28.0, 28.4 (2 × CMe_3), 51.7, 53.3, 53.5 (3 × *C*(1)), 54.5, 55.8, 56.1 (3 × *C*(2)), 80.1, 80.3 (2 × *C*Me$_3$), 156.5 (N*C*O [carbamate]), 173.1, 174.3 (2 × N*C*O [amide], $CO_2{}^tBu$); *m*/*z* (ESI^+) 530 ($[M+Na]^+$, 100%) 509 ($[M+H]^+$, 25%); HRMS (ESI^+) $C_{27}H_{46}N_3O_6{}^+$ ($[M+H]^+$) requires 508.3381; found 508.3385.

4.20. Boc-[(*S*,*S*)-ACPC]$_4$-O^{t}Bu 27

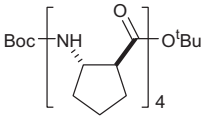

Following General Procedure 4, **20** (76.2 mg, 0.12 mmol), Boc_2O (28.0 mg, 0.13 mmol) and $Pd(OH)_2$/C (50% w/w substrate, 38.1 mg) in MeOH (10 mL) gave, after purification via recrystallisation ($CHCl_3$/heptane), **27** as a white solid (47.0 mg, 65%, >99:1 dr); mp 233–235 °C (dec); $[\alpha]_D^{23} = +48.7$ (*c* 0.4 in $CHCl_3$); ν_{max} (2 mM solution in $CHCl_3$) 3438, 3340, 3273 (N–H); ν_{max} (KBr) 3300 (N–H), 1720, 1690, 1647, 1553 (C=O); δ_H (400 MHz, $CDCl_3$, 26 mM) 1.36–2.18 (24H, m, 4 × C(3)H_2, 4 × C(4)H_2, 4 × C(5)H_2) overlapping 1.43 (9H, s, CMe_3) and 1.45 (9H, s, CMe_3), 2.42–2.49 (2H, m, 2 × C(1)*H*), 2.55–2.63 (1H, m, C(1)*H*), 2.62–2.69 (1H, m, C(1)*H*), 3.90–4.01 (1H, m, C(2)*H*), 4.14–4.25 (2H, m, 2 × C(2)*H*), 4.36–4.45 (1H, m, C(2)*H*), 4.80 (1H, d, *J* 7.2, N*H*), 7.33 (1H, d, *J* 7.5, N*H*), 7.98 (1H, d, *J* 6.8, N*H*), 8.09 (1H, d, *J* 7.5, N*H*); δ_C (100 MHz, $CDCl_3$) 23.4, 23.7, 24.5, 27.5, 28.1, 28.6, 30.9, 32.8, 33.3, 33.3, 33.6 (4 × *C*(3), 4 × *C*(4), 4 × *C*(5)), 28.0, 28.4 (2 × CMe_3), 51.5, 52.7, 53.5, 53.6 (4 × *C*(1)), 54.4, 55.4, 55.5, 56.5 (4 × *C*(2)), 80.0, 80.1 (2 × *C*Me$_3$), 156.3 (N*C*O [carbamate]), 173.4, 174.4, 174.6 (3 × N*C*O [amide], $CO_2{}^tBu$); *m*/*z* (ESI^+) 619 ($[M+H]^+$, 92%), 563 ($[M-C_4H_9]^+$, 100%); HRMS (ESI^+) $C_{33}H_{54}N_4NaO_7{}^+$ ($[M+Na]^+$) requires 641.3885; found 641.3881.

4.20.1. X-ray crystal structure determination for 27

Data were collected using an Enraf-Nonius κ-CCD diffractometer with graphite monochromated Mo Kα radiation using standard procedures at 190 K. The structure was solved by direct methods (SIR92); all non-hydrogen atoms were refined with anisotropic

thermal parameters. Hydrogen atoms were added at idealised positions. The structure was refined using CRYSTALS.[26]

X-ray crystal structure data for **27** [$C_{33}H_{54}N_4O_7$]: M = 618.81, triclinic, space group *P1*, a = 9.3085(3) Å, b = 9.2742(3) Å, c = 11.2806(6) Å, α = 93.1887(17)°, β = 93.0542(17)°, γ = 113.577(2)°, V = 888.13(6) Å^3, Z = 1, μ = 0.081 mm^{-1}, colourless plate, crystal dimensions = 0.1 × 0.1 × 0.3 mm^3. A total of 3520 unique reflections were measured for 5 < θ < 27 and 2585 reflections were used in the refinement. The final parameters were wR_2 = 0.101 and R_1 = 0.077 [I >2.0σ(I)].

Crystallographic data (excluding structure factors) have been deposited with the Cambridge Crystallographic Data Centre as supplementary publication number CCDC 772472. Copies of the data can be obtained, free of charge, on application to CCDC, 12 Union Road, Cambridge CB2 1EZ, UK [fax: +44(0) 1223 336033 or e-mail: deposit@ccdc.cam.ac.uk].

4.21. Boc-[(*S*,*S*)-ACPC]$_5$-O^{t}Bu 28

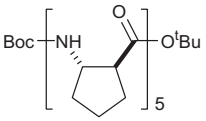

Following General Procedure 4, **23** (173 mg, 0.23 mmol), Boc_2O (54.5 mg, 0.25 mmol) and $Pd(OH)_2/C$ (25% by wt, 86.7 mg) in MeOH (20 mL) gave, after purification via recrystallisation ($CHCl_3$/heptane), **28** (101 mg, 61%, >99:1 dr) as a white solid; mp 230–232 °C ($CHCl_3$/heptane); $[\alpha]_D^{23}$ = +45.8 (*c* 0.6 in $CHCl_3$); ν_{max} (2 mM solution in $CHCl_3$) 3436, 3336 (N–H); δ_H (400 MHz, $CDCl_3$, 26 mM) 1.30–2.18 (30H, m, 5 × C(3)H_2, 5 × C(4)H_2, 5 × C(5)H_2) overlapping 1.44 (18H, app s, 2 × CMe_3), 2.21–2.68 (4H, m, 4 × C(1)*H*), 2.72–2.84 (1H, m, C(1)*H*), 3.92–4.07 (1H, m, C(2)*H*), 4.14–4.34 (3H, m, 3 × C(2)*H*), 4.36–4.50 (1H, m, C(2)*H*), 5.09 (1H, d, *J* 7.5, N*H*), 6.74 (1H, d, *J* 7.5, N*H*), 7.65 (1H, d, *J* 8.2, N*H*), 8.15 (1H, d, *J* 7.2, N*H*), 8.20 (1H, d, *J* 7.2, N*H*); δ_C (100 MHz, $CDCl_3$) 23.4, 23.5, 24.6, 24.8, 27.9, 28.1, 28.8, 28.9, 32.7, 33.2, 33.4, 33.5 (5 × *C*(3), 5 × *C*(4), 5 × *C*(5)), 28.0, 28.4 (2 × C*Me*$_3$), 51.3, 52.4, 52.5, 53.3, 54.1, 54.3, 55.3, 55.4, 56.9 (5 × *C*(1), 5 × *C*(2)), 79.9 (2 × C*Me*$_3$), 156.2 (N*C*O [carbamate]), 174.1, 174.4, 174.6, 174.9 (4 × N*C*O [amide], *C*O$_2$^{t}Bu); *m*/*z* (ESI$^+$) 789 ([M+NH$_4$+MeCN]$^+$, 52%), 752 ([M+Na]$^+$, 89%), 730 ([M+H]$^+$, 100%); HRMS (ESI$^+$) $C_{39}H_{63}N_5NaO_8^+$ ([M+Na]$^+$) requires 752.4569; found 752.4557.

4.21.1. X-ray crystal structure determination for 28

Data were collected using an Enraf-Nonius κ-CCD diffractometer with graphite monochromated Mo Kα radiation using standard procedures at 190 K. The structure was solved by direct methods (SIR92); all non-hydrogen atoms were refined with anisotropic thermal parameters. Hydrogen atoms were added at idealised positions. The structure was refined using CRYSTALS.[26]

X-ray crystal structure data for **28** [$C_{39}H_{63}N_5O_8$]: M = 729.96, monoclinic, space group $P2_1$, a = 9.1420(3) Å, b = 19.7069(5) Å, c = 11.6211(4) Å, β = 92.5033(12)°, V = 2091.67(11) Å^3, Z = 2, μ = 0.81 mm^{-1}, colourless plate, crystal dimensions = 0.1 × 0.2 × 0.3 mm^3. A total of 4852 unique reflections were measured for 5 < θ < 27 and 2848 reflections were used in the refinement. The final parameters were wR_2 = 0.085 and R_1 = 0.071 [I >1.9σ(I)].

Crystallographic data (excluding structure factors) have been deposited with the Cambridge Crystallographic Data Centre as supplementary publication number CCDC 772473. Copies of the data can be obtained, free of charge, on application to CCDC, 12 Union Road, Cambridge CB2 1EZ, UK [fax: +44(0) 1223 336033 or e-mail: deposit@ccdc.cam.ac.uk].

4.22. Boc-[(*S*,*S*)-ACPC]$_6$-O^{t}Bu 29

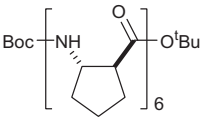

Following General Procedure 4, **24** (120 mg, 0.14 mmol), Boc_2O (36.0 mg, 0.17 mmol) and $Pd(OH)_2/C$ (25% w/w substrate, 60.2 mg) in MeOH (10 mL) gave the crude reaction mixture. The residue was dissolved in MeOH (60 mL), $NaHCO_3$ (12.3 mg, 0.15 mmol) was added and the mixture was allowed to stand in an ultrasonic bath for 24 h at rt. The reaction mixture was then diluted with $CHCl_3$ (100 mL) and washed sequentially with 1 M aq HCl (2 × 100 mL) and brine (100 mL), then dried and concentrated in vacuo. Purification via flash column chromatography (gradient elution, 0→18% MeOH in $CHCl_3$) gave **29** as a white crystalline solid (27.6 mg, 23%, >99:1 dr); R_f 0.04 ($CHCl_3$/MeOH, 20:1); mp 250–251 °C; $[\alpha]_D^{20}$ = +48.7 (*c* 1.1 in $CHCl_3$); ν_{max} (2 mM solution in $CHCl_3$) 3439, 3326 (N–H); δ_H (400 MHz, $CDCl_3$, 26 mM) 1.31–2.53 (40H, m, 4 × C(1)*H*, 6 × C(3)H_2, 6 × C(4)H_2, 6 × C(5)H_2) overlapping 1.43 (9H, s, CMe_3) and 1.44 (9H, s, CMe_3), 2.60–2.71 (1H, m, C(1)*H*), 2.80–2.91 (1H, m, C(1)*H*), 3.98–4.31 (1H, m, C(2)*H*), 4.20–4.31 (4H, m, 4 × C(2)*H*), 4.37–4.43 (1H, m, C(2)*H*), 5.62 (1H, d, *J* 8.9, N*H*), 6.86 (1H, d, *J* 8.2, N*H*), 7.61 (1H, d, *J* 9.2, N*H*), 8.25–8.35 (2H, m, 2 × N*H*), 8.40 (1H, d, *J* 7.5, N*H*); δ_C (125 MHz, $CDCl_3$) 23.3, 23.5, 24.5, 24.7, 25.0, 28.2, 28.3, 28.9, 29.3, 29.7, 32.6, 33.2, 33.4, 33.5 (6 × *C*(3), 6 × *C*(4), 6 × *C*(5)), 28.1, 28.5 (2 × C*Me*$_3$), 51.2, 52.1, 52.3, 52.3, 53.0 (6 × *C*(1)), 54.3, 55.2, 55.3, 57.2 (6 × *C*(2)), 79.7, 79.9 (2 × C*Me*$_3$), 156.2 (N*C*O [carbamate]), 174.3, 174.5, 174.5, 174.8, 175.1 (5 × N*C*O [amide], *C*O$_2$^{t}Bu); *m*/*z* (ESI$^+$) 864 ([M+Na]$^+$, 84%), 842 ([M+H]$^+$, 100%); HRMS (ESI$^+$) $C_{45}H_{73}N_6O_9^+$ ([M+H]$^+$) requires 841.5434; found 841.5434.

4.22.1. X-ray crystal structure determination for 29

Data were collected using an Enraf-Nonius κ-CCD diffractometer with graphite monochromated Mo Kα radiation using standard procedures at 190 K. The structure was solved by direct methods (SIR92); all non-hydrogen atoms were refined with anisotropic thermal parameters. Hydrogen atoms were added at idealised positions. The structure was refined using CRYSTALS.[26]

X-ray crystal structure data for **29** [$C_{45}H_{72}N_6O_9$]: M = 841.10, tetragonal, space group $P4_3$, a = 10.3345(2) Å, b = 10.3358(2) Å, c = 44.0581(9) Å, V = 4706.08(16) Å^3, Z = 4, μ = 0.083 mm^{-1}, colourless block, crystal dimensions = 0.2 × 0.2 × 0.2 mm^3. A total of 4699 unique reflections were measured for 5 < θ < 27 and 4120 reflections were used in the refinement. The final parameters were wR_2 = 0.178 and R_1 = 0.106 [I >−3.0σ(I)].

Crystallographic data (excluding structure factors) have been deposited with the Cambridge Crystallographic Data Centre as supplementary publication number CCDC 772474. Copies of the data can be obtained, free of charge, on application to CCDC, 12 Union Road, Cambridge CB2 1EZ, UK [fax: +44(0) 1223 336033 or e-mail: deposit@ccdc.cam.ac.uk].

4.23. Cbz-[(*S*,*S*)-ACPC]$_3$-OH 30

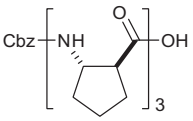

Following General Procedure 2, **19** (250 mg, 0.46 mmol) and TFA (0.70 mL) in CH_2Cl_2 (2.10 mL) gave, after purification via trituration with Et_2O, **30** as a white solid (171 mg, 76%, >99:1 dr); mp

213–215 °C; $[\alpha]_D^{23} = +29.1$ (*c* 0.3 in MeOH); ν_{max} (KBr) 3313 (N–H, O–H), 1706, 1649, 1560 (C=O); δ_H (400 MHz, $CDCl_3$) 1.23–2.31 (18H, m, 3 × C(3)H_2, 3 × C(4)H_2, 3 × C(5)H_2), 2.34–2.51 (2H, m, 2 × C(1)*H*), 2.89–2.99 (1H, m, C(1)*H*), 3.94–4.14 (2H, m, 2 × C(2)*H*), 4.15–4.27 (1H, m, C(2)*H*), 5.00 (1H, d, *J* 7.2, N*H*), 5.08 (1H, d, *J* 12.3, CH_AH_BPh), 5.13 (1H, d, *J* 12.3, CH_AH_BPh), 6.89 (1H, d, *J* 7.9, N*H*), 7.31–7.45 (5H, m, *Ph*), 8.58 (1H, br s, N*H*); δ_C (125 MHz, $CDCl_3$) 23.9, 24.2, 25.4, 28.0, 28.0, 28.2, 33.0, 33.2, 33.7 (3 × *C*(3), 3 × *C*(4), 3 × *C*(5)), 53.0, 53.2, 53.5 (3 × *C*(1)), 55.4, 55.7, 57.2 (3 × *C*(2)), 67.2 (*C*H_2Ph), 128.0, 128.4, 128.6 (*o*,*m*,*p*-*Ph*), 136.0 (*i*-*Ph*), 156.6 (*NC*O [carbamate]), 174.5, 175.3, 177.0 (2 × *NC*O [amide], *C*O_2H); *m*/*z* (ESI^+) 545 ([M+NH_4+MeCN]$^+$, 15%), 508 ([M+Na]$^+$, 100%), 486 ([M+H]$^+$, 60%); HRMS (ESI^+) $C_{26}H_{35}N_3NaO_6^+$ ([M+Na]$^+$) requires 508.2418; found 508.2417.

4.23.1. X-ray crystal structure determination for 30

Data were collected using an Enraf-Nonius κ-CCD diffractometer with graphite monochromated Mo Kα radiation using standard procedures at 190 K. The structure was solved by direct methods (SIR92); all non-hydrogen atoms were refined with anisotropic thermal parameters. Hydrogen atoms were added at idealised positions. The structure was refined using CRYSTALS.[26]

X-ray crystal structure data for **30** [$C_{26}H_{35}N_3O_6$]: $M = 485.58$, tetragonal, space group $P4_1$, $a = 10.15760(10)$ Å, $c = 24.3046(5)$ Å, $V = 2507.67(6)$ Å^3, $Z = 4$, $\mu = 0.092$ mm^{-1}, colourless plate, crystal dimensions = 0.2 × 0.2 × 0.3 mm^3. A total of 2908 unique reflections were measured for $5 < \theta < 27$ and 2360 reflections were used in the refinement. The final parameters were $wR_2 = 0.056$ and $R_1 = 0.046$ [$I > 2.5\sigma(I)$].

Crystallographic data (excluding structure factors) have been deposited with the Cambridge Crystallographic Data Centre as supplementary publication number CCDC 772475. Copies of the data can be obtained, free of charge, on application to CCDC, 12 Union Road, Cambridge CB2 1EZ, UK [fax: +44(0) 1223 336033 or e-mail: deposit@ccdc.cam.ac.uk].

References

1. (a) Seebach, D.; Overhand, M.; Kuhnle, F. N. M.; Martinoni, B.; Oberer, L.; Hommel, U.; Widmer, H. *Helv. Chim. Acta* **1996**, *79*, 913; (b) Hintermann, T.; Seebach, D. *Chimia* **1997**, *50*, 244; (c) Seebach, D.; Abele, S.; Schreiber, J. V.; Martinoni, B.; Nussbaum, A. K.; Schild, H.; Schulz, H.; Hennecke, H.; Woessner, R.; Bitsch, F. *Chimia* **1998**, *52*, 734; (d) Seebach, D.; Hook, D. F.; Glätti, A. *Biopolymers (Peptide Science)* **2006**, *84*, 23.; (e) Aguilar, M.-I.; Purcell, A. W.; Devi, R.; Lew, R.; Rossjohn, J.; Smith, I.; Perlmutter, P. *Org. Biomol. Chem.* **2007**, *5*, 2884.
2. Werder, M.; Hauser, H.; Abele, S.; Seebach, D. *Helv. Chim. Acta* **1999**, *82*, 1774.
3. Hamuro, Y.; Schneider, J. P.; DeGrado, W. F. *J. Am. Chem. Soc.* **1999**, *121*, 12200; Liu, D.; DeGrado, W. F. *J. Am. Chem. Soc.* **2001**, *123*, 7553.
4. For instance, see: Hintermann, T.; Seebach, D. *Synlett* **1997**, 437; Seebach, D.; Abele, S.; Gademann, K.; Guichard, G.; Hintermann, T.; Jaun, B.; Matthews, J. L.; Schreiber, J. V. *Helv. Chim. Acta* **1998**, *81*, 932; Gung, B. W.; Zou, D. *J. Org. Chem.* **1999**, *64*, 2176; Raguse, L.; Lai, J. R.; Gellman, S. H. *Helv. Chim. Acta* **2002**, *85*, 4154; Glättli, A.; Seebach, D.; van Gunsteren, W. F. *Helv. Chim. Acta* **2004**, *87*, 24872; Luppi, G.; Galeazzi, R.; Garavelli, M.; Formaggio, F.; Tomasini, C. *Org. Biomol. Chem.* **2004**, *2*, 2187; Izquierdo, S.; Kogan, M. J.; Parella, T.; Moglioni, A. G.; Branchadell, V.; Giralt, E.; Ortuño, R. M. *J. Org. Chem.* **2004**, *69*, 5093.
5. The *n*-helix nomenclature is used to define the C=O···H–N hydrogen bonded ring sizes observed within the peptide backbone.
6. In contrast, it is often noted that α-peptides usually require at least 15 residues to elicit any noticeable conformational preferences; see: Quinkirt, G.; Egert, E.; Griesinger, C. In *Peptides: Synthesis, Structure, and Applications*; Gutte, B., Ed.; Academic Press: San Diego, 1995.
7. (a) Appella, D. H.; Christianson, L. A.; Karle, I. L.; Powell, D. R.; Gellman, S. H. *J. Am. Chem. Soc.* **1996**, *118*, 13071; (b) Barchi, J. J., Jr.; Huang, X.; Appella, D. H.; Christianson, L. A.; Durell, S. R.; Gellman, S. H. *J. Am. Chem. Soc.* **2000**, *122*, 2711.
8. Appella, D. H.; Christianson, L. A.; Klein, D. A.; Powell, D. R.; Huang, X.; Barchi, J. J., Jr.; Gellman, S. H. *Nature* **1997**, *387*, 381; Applequist, J.; Bode, K. A.; Appella, D. H.; Christianson, L. A.; Gellman, S. H. *J. Am. Chem. Soc.* **1998**, *120*, 4891.
9. The ability to adopt alternative conformations is a consequence of the relationship between alkyl ring size and torsional angle θ. Transhexacin favours a torsional angle θ of around 60°, which specifically stabilises the 14-helix, whereas the smaller ring size of transpentacin biases θ towards larger values, rendering the 12-helix the most favourable conformer, see: Banerjee, A.; Balaram, P. *Curr. Sci.* **1997**, *73*, 1067.
10. For instance, see: Wang, X.; Espinosa, J. F.; Gellman, S. H. *J. Am. Chem. Soc.* **2000**, *122*, 4821; Lee, H.-S.; Syud, F. A.; Wang, X.; Gellman, S. H. *J. Am. Chem. Soc.* **2001**, *123*, 7721; Winkler, J. D.; Piatnitski, E. L.; Mehlmann, J.; Kasparec, J.; Axelsen, P. H. *Angew. Chem., Int. Ed.* **2001**, *40*, 743; Woll, M. G.; Fisk, J. D.; LePlae, P. R.; Gellman, S. H. *J. Am. Chem. Soc.* **2002**, *124*, 12447; Raguse, L.; Lai, J. R.; Gellman, S. H. *J. Am. Chem. Soc.* **2003**, *125*, 5592; Park, J.-S.; Lee, H.-S.; Lai, J. R.; Kim, B. M.; Gellman, S. H. *J. Am. Chem. Soc.* **2003**, *125*, 8539; Peelen, T. J.; Chi, Y.; English, E. P.; Gellman, S. H. *Org. Lett.* **2004**, *6*, 4411; Simpson, G. L.; Gordon, A. H.; Lindsay, D. M.; Promsawan, N.; Crump, M. P.; Mulholland, K.; Hayter, B. R.; Gallagher, T. *J. Am. Chem. Soc.* **2006**, *128*, 10638; Martinek, T. A.; Mándity, I. M.; Fülöp, L.; Tóth, G. K.; Vaas, E.; Hollósi, M.; Forró, E.; Fülöp, F. *J. Am. Chem. Soc.* **2006**, *128*, 13539.
11. Throughout this manuscript, the cyclopentane rings are represented as puckered on C(2) for clarity; however, a conformational preference is not implied.
12. (a) Davies, S. G.; Ichihara, O.; Walters, I. A. S. *Synlett* **1993**, 461; (b) Davies, S. G.; Ichihara, O.; Lenoir, I.; Walters, I. A. S. *J. Chem. Soc., Perkin Trans. 1* **1994**, 1411; α,β-Unsaturated ester **10** was synthesised by an analogous procedure to that outlined by Davies, S. G.; Garner, A. C.; Long, M. J. C.; Smith, A. D.; Sweet, M. J.; Withey, J. M. *Org. Biomol. Chem.* **2004**, *2*, 3355.
13. Recrystallisation of an aliquot gave a sample of **11** in >99:1 dr that was subjected to single crystal X-ray analysis, thus unambiguously confirming the relative *cis*-configuration, with the absolute (1*R*,2*S*,α*S*)-configuration being assigned from the known (*S*)-configuration of the α-methylbenzyl stereocentre.
14. The presence of water resulted in partial hydrolysis of the *tert*-butyl ester, thought to arise through the in situ production of potassium hydroxide. This phenomenon was also observed by McErlean, C. S. P.; Moody, C. J. *J. Org. Chem.* **2007**, *72*, 10298.
15. Single crystal X-ray analysis of **12** unambiguously confirmed the *trans*-relative configuration, with the absolute (*S*,*S*,*S*)-configuration being assigned from the known (*S*)-configuration of the α-methylbenzyl stereocentre.
16. Single crystal X-ray analysis of **15** unambiguously confirmed the relative *trans*-configuration, indicating that the stereochemical integrity of the molecule was not compromised using this protecting group strategy. The absolute (*S*,*S*)-configurations within **13**, **14** and **15** could therefore also be confidently assigned from the known absolute configurations of **11** and **12**.
17. A sample of trimer acid **30** was prepared via treatment of trimer **19** with TFA in CH_2Cl_2.
18. Structures were overlaid using the Chem-3D structure mapping function.
19. This procedure took advantage of the fact that the C-terminus C(1)*H* proton forms just one short-range NOE correlation to one N*H* proton, when all remaining C(1)*H* protons form short-range NOE correlations to two N*H* protons. Similarly the N-terminus N*H* proton forms just one short-range NOE correlation to one C(1)*H* proton when all remaining N*H* protons form short-range NOE correlations to two C(1)*H* protons; see Ref. 7b.
20. NMR structure calculations for all the transpentacin oligomers was performed using the XPLOR software package (Brünger, A.T. *XPLOR Version 3.1: A system for X-ray crystallography and NMR*, Yale University Press, New Haven CT, 1992) with the parameter and topology files modified so they are appropriate for β-amino acids. For each peptide the NOE intensities were categorised as either very strong, strong, medium, weak or very weak. The corresponding distance restraints used in the structure calculations for the five categories were 1.8–2.5 Å (very strong), 1.8–3.0 Å (strong), 1.8–3.5 Å (medium), 1.8–4.0 Å (weak) and 1.8–5.0 Å (very weak). Pseudoatoms were used in the structure calculations where no stereospecific assignments have been made. Where hydrogen bond restraints were used in the structure refinement, the distance restraints used were NH(i)-O(j), 1.3–2.3 Å and N(i)-O(j), 2.3–3.3 Å. A simulated annealing protocol was used with ensembles of 20 structures being calculated and the lowest energy 10 structures used for analysis.
21. Nilges, M.; Gronenborn, A. M.; Brunger, A. T.; Clore, G. M. *Protein Eng.* **1988**, *2*, 27.
22. Pangborn, A. B.; Giardello, M. A.; Grubbs, R. H.; Rosen, R. K.; Timmers, F. J. *Organometallics* **1996**, *15*, 1518.
23. Gung, B. W.; Zou, D.; Stalcup, A. M.; Cottrell, C. E. *J. Org. Chem.* **1999**, *64*, 2176.
24. Babler, J. H.; Sarusi, S. J. *J. Org. Chem.* **1987**, *52*, 3462.
25. Henderson, D.; Richardson, K. A.; Taylor, R. J. K.; Saunders, J. *Synthesis* **1983**, *12*, 996.
26. Betteridge, P. W.; Carruthers, J. R.; Cooper, R. I.; Prout, C. K.; Watkin, D. J. CRYSTALS, 2001, Issue 11, Chemical Crystallography Laboratory, University of Oxford: UK.